BIOCHEMICAL AND FUNCTIONAL CHARACTERIZATION OF CUTIN SYNTHASE 2 FROM TOMATO (*SOLANUM LYCOPERSICUM*)

A Thesis

Presented to the Faculty of the Graduate School

of Cornell University

In Partial Fulfillment of the Requirements for the Degree of

Master of Science

by

Nicholas Adam Segerson

December 2018

ABSTRACT

Cutin synthase-like (CUS) proteins comprise a family of GDSL esterase/lipases that catalyze the polymerization of cutin, a major component of plant cuticles. The best characterized example, SLCUS1 from tomato (*Solanum lycopersicum*), has been shown to polymerize extracellular cutin during fruit expansion and some aspects of its enzymatic activity *in vitro* have been described. However, fruit from the *slcus1* mutant, which does not express *SLCUS1*, still accumulate a thin layer of polymeric cutin, indicating there are other enzymes or mechanisms that contribute to cutin polymerization in tomato fruit. Here it is reported that *SLCUS2*, an ortholog of *SLCUS1*, is also expressed in fruit, albeit to a lesser degree than *SLCUS1*, and is a likely candidate for contribute to the formation of the polymeric cutin detected in *slcus1* fruit. *SLCUS2* is predominantly expressed earlier in fruit development than *SLCUS1*, coincident with cutin deposition, as well as in floral tissues. SLCUS2 was expressed in a heterologous system and mass spectrometric analysis of the products of the enzyme indicated that it catalyzes the polymerization of cutin *in vitro*. No differences in the products of SLCUS2 and SLCUS1 could be detected using the techniques in this study. Furthermore, no differences in the products upon co-incubation of SLCUS1 and SLCUS2 could be detected. Michaelis-Menten kinetics were determined for SLCUS2 and were found to have comparable kinetics to SLCUS1, with a slower turnover rate. To elucidate the role of the enzyme *in planta*, null *SLCUS2* mutant lines

were generated using CRISPR/Cas9 vectors which resulted in a truncated protein. However, no significant changes in polymeric cutin levels, distribution or composition were observed in either the fruits or flowers. While SLCUS2 is able to polymerize cutin, the role of the enzyme *in planta* could not be determined in this study. Further work may result in determine the *in planta* role of SLCUS2 including generating double mutants with *slcus1* and the use of techniques which can determine architectural differences in the cutin polymer of *slcus2* fruits.

BIOGRAPHICAL SKETCH

Nicholas Segerson was born in Mesa, Arizona to Valerie and Charles Segerson. He was raised in Tempe Arizona alongside one, younger sister Kelly. He graduated from Corona del Sol High School in 2009 and enrolled in Arizona State University. He graduated from Arizona State University with a Bachelors of Science degree in 2009. While there, he worked with Dr. Tsafrir Mor as part of the Center of Membrane Proteins in Infectious Diseases (MPID). He joined the Plant Biology program in 2013, where he joined Dr. Jocelyn Rose's lab.

ACKNOWLEDGMENTS

First and foremost, I would like to thank my advisor, Joss Rose. He took me into his lab and offered me an array of opportunities and learning experiences. I would also like to thank the rest of my committee, Jim Giovannoni and Karl Niklas who have provided many useful insights during my time at Cornell. My fellow Rose lab members, past and present, have also been an immense help both in research and in keeping spirits high.

I would like to thank my family, my parents Chuck and Val Segerson, who through hard work and careful thought are responsible for the person that I have become today. I also think of my sister Kelly, who I share many wonderful memories of our childhood with. My grandparents, Murial and John Segerson and Patsie and Robert Bejar who always offered their warm, welcoming homes no matter what. Of course, I cannot forget the innumerable Aunts, Uncles, and Cousins who have always been there for me. If it were possible, I would write a second thesis just to include them all.

The friends that I've met during graduate school have also been pillars of support on which I have leaned during difficult times. Michael Zarfos, Charlotte Levy, Zoe Getman-Pickering, Adam Campbell, Angela Kruse, and Chris Peritore Galve, thank you for always lending a sympathetic ear. I will always cherish our time together and the adventures we've shared. Once again, I apologize that I cannot list everyone who has made an impact on my time here, but our friendship will always be special to me.

And finally, Julia Miller, who has helped to prop me up while I was at my needed you the most. I couldn't have done this without your love and support. I look forward to our futures together.

TABLE OF CONTENTS

CHAPTER 1

Introduction

Sequence to Structure

Lipases (EC 3.1.1.3) and esterases (EC 3.1.1.1) are families of enzymes that catalyze the hydrolysis of carboxylic ester bonds. Initially, the two families were differentiated by a feature that some lipases exhibited called “interfacial activation”, which resulted in an increase in activity at the interface between a lipid monolayer and water (Verger, 1997). This distinction was not sufficient however, as this feature was not present in all lipases. More recent distinctions define lipases as enzymes that preferentially hydrolyze long chain acylglycerols (≥10 carbon atoms), while esterases hydrolyze short chain acylglycerols (≤ 10 carbon atoms) (Chahinian *et al.*, 2002). Both families possess wide substrate specificity and, in some cases, additional activities, such as phospholipase, cholesterol esterase, and amidase activities (Svendsen, 2000).

Both families can be further categorized as α/ β hydrolases, which possess a catalytically active serine, typically found in the middle of the primary amino acid sequence in the motif: GxSxG, where x is any amino acid. Structurally, α/ β hydrolases are characterized by eight β-sheets, all but one of which orient in the parallel direction. In addition, most of these enzymes have six α-helices arranged at the sides of the β-sheets (Akoh *et al.*, 2004).

In 1995, a subfamily of hydrolases that differed from canonical hydrolases was identified (Upton and Buckley, 1995), in that the catalytic

serine was located closer to the N-terminus of the primary amino acid sequence in the motif: GDSL. This GDSL subfamily can be further classified as SGNH hydrolases, named for four highly conserved amino acid residues found in distinct conserved blocks throughout the sequence. First, the catalytic serine (S), located near the N-terminus which, along with another two residues toward the C-terminus, make up the catalytic triad. The second two residues (G and N), form the oxyanion hole, and act to stabilize the intermediate formed during catalysis through the formation of hydrogen bonds between these residues and the substrate (Pleiss *et al.*, 2000). The final residue (H) is believed to increase the nucleophilic capability of the catalytic serine by deprotonating the residue's hydroxyl group.

While members of the GDSL family have been identified in all kingdoms of life, those in bacteria have been the most characterized. The first GDSL crystal structure was solved was from *Streptomyces scabies* (Wei *et al.*, 1995). Though the GDSL family had yet to be described, the authors did note that the structure differed greatly from previously reported esterase and lipase structures, setting the foundation for future characterization. Crystal structures of GDSL enzymes from *Escherichia coli* (Li *et al.*, 2000; Lo *et al.*, 2000; Lo *et al.,* 2003)*, Pseudomonas fluorescens* (Cheeseman *et al.*, 2004)*, Mycobacterium smegmatis* (Matthews *et al.*, 2007)*, and Pseudomonas aeruginosa* (van den Berg, 2010) have also been solved. To date, the only GDSL structures that have been solved have been from bacterial sources. Also of note, the crystal structures that have been solved thus far lack a lid; a

structural feature that requires conformational changes in the enzyme before catalysis can occur, which is common to most lipases (Khan *et al.*, 2001).

Perhaps the most well characterized GDSL enzyme has been thioesterase/protease I (TEP-I) from *E. coli* (Lo *et al.*, 2003). Solving the crystal structure, along with the use of nuclear magnetic resonance (NMR) analysis revealed that the catalytically active serine is present on a rigid portion of the enzyme, while the other two residues in the catalytic triad are located in flexible portions (Huang *et al.*, 2001). As all three residues of the catalytic triad are required for catalysis, conformational changes of TEP-I would be required in order for the enzyme to become active, likely upon interaction with a substrate. This flexible site has been hypothesized to explain the wide substrate specificity of TEP-I and the GDSL superfamily in general (Akoh et al., 2005). However, a wider breadth of GDSL protein structures is needed to confirm the degree to which this is true for other members of the family.

Industrial Interest in GDSL enzymes

There has been much interest in the use of both lipases and esterases for industrial purposes, due in part the range of substrates and resilience of the enzymes. In 2008, the industrial enzyme market had a worldwide value of $4.7 billion dollars; however, this value was expected to increase to by an average of 6.3% annually (CDBM, 2008; Freedonia, 2009). Of the entire industrial enzyme market, lipases are the third most important group of

enzymes for the market, after proteases and carbohydrases (Hasan *et al.*, 2005). While the uses vary, depending on the associated industry, generally speaking, members of the GDSL superfamily are utilized for their wide substrate pools and their ability to remain functional in biochemically challenging conditions. Production of these enzymes for industrial purposes is typically based on microbial systems, involving submerged fermentation (Ito *et al.*, 2001).

In food processing, the enzymes are often used as emulsifying agents and to modify food products to be more flavorful. One such example is in the production of enzyme-modified cheese, which can be used to create cheese powders and cheese flavoring (Kilcawley *et al.*, 2005). In additions, many high fructose corn syrups are produced using esterases to hydrolyze corn starches (Houde *et al.*, 2003).

In medicine, hydrolases are used to produce single enantiomers of drugs to avoid potential negative side effects of racemic mixtures. The classes of drugs produced by hydrolases are wide and include anti-cancer drugs, anti-Alzheimer drugs, and common over-the-counter drugs, such as ibuprofen (Houde *et al.,* 2003). In addition, the broad specificity provided by hydrolases make them strong candidates for the production of novel drugs (Peterson *et al.*, 2001).

Finally, hydrolases are used in the detergent and laundering industry, where their ability to remain active at high temperatures and in basic pHs solutions are valued. Lipolase® was the first recombinant enzyme to be

introduced to market for laundering purposes. The enzyme has an optimal pH range of 10.5 to 11.0 and an optimum temperature of 40°C. Since the introduction of these enzymes, detergent enzymes have grown to account for as much as 30% of the entire enzyme market (Pandey *et al.*, 1999).

Plant GDSL proteins

While many GDSL enzymes have been fairly well characterized in bacteria; less is known about those from plants. The GDSL esterase/lipase superfamily in plants is large, often with over 100 members per species. This has been reported to have arisen through gene duplication events over time (Chepyshko *et al.*, 2012). For instance, 108 members have been identified in *Arabidopsis thaliana*, while *Oryza sativa* has 114 members, *Zea mays* has 53, *Chlamydomonas reinhardtii* has 102, and *Physcomitrella patens* has 57 (Ling 2008; Volokita *et al.*, 2010; Youens-Clark *et al.*, 2010; Ouyang *et al.*, 2010).

With a wealth of genomic information becoming more available, researchers have attempted to group GDSL enzymes from species such as *A. thaliana* and *O. sativa* by predicted functions using functionally characterized orthologs, while others have identified putative motifs unique in subgroups within the superfamily (Chepyshko *et al.,* 2012; Dong *et al.*, 2016). One limitation of this method is that few of the plant GDSL enzymes have known native substrates. As such, much of our understanding of these proteins relies on the characterization of overexpression and knockout mutants, often without the identification of a specific mechanism. To this end, GDSL enzymes in

plants have been associated with a wide range of functions, including the synthesis of secondary metabolites, defense responses, and developmental processes, as summarized below.

One of the most widely attributed functions of plant GDSL enzymes is in defense responses, either in the formation of defense compounds, or through mechanisms that are not yet understood. In one study, researchers used recombinant inbred lines between two *A. thaliana* ecotypes Colmbia and Landsburg *erecta* and identified a quantitative trait locus (QTL) which caused plants to accumulate less nitriles and more isothiocyanates. The gene underlying the QTL was identified as a GDSL, EPITHIOSPECIFIER MODIFIER1 (ESM1) (Zhang *et al.*, 2006), although the mechanism of action is not yet known. *MODIFIED VACUOLE PHENOTYPE1* (*MVP1*), was also found to be involved in the glucosinolate hydrolysis process; however, no direct chemical mechanism could be attributed although the authors hypothesize that the enzyme is responsible for localizing other enzymes which catalyze glucosinolate hydrolysis (Agee *et al.*, 2010). Notably, *MVP1* has a GDGL, rather than the canonical GDSL, motif which diverges from other members of the family. The serine residue is required to catalyze lipolytic reactions as evidenced in multiple site-directed mutagenesis studies (Yeats *et al.,* 2011) and the authors confirmed that *MVP1* lacks lipase activity.

In some situations, GDSL enzymes have been implicated in defense responses even when no direct function can be attributed. GDSL LIPASE1 (GLIP1) was found to disrupt fungal spore formation and knockout lines had

altered expression of both defense and ethylene response genes and an increased susceptibility to the fungus *Alternaria brassicicola*, suggesting a role in defense regulation (Oh *et al.*, 2005; Kwon *et al.*, 2009). *GLIP2*, an ortholog of *GLIP1*, is expressed in roots and its expression is induced by the application of various hormones, including ethylene. *GLIP2* expression was found to increase resistance to a necrotrophic bacterium, *Erwinia carotovora,* by suppressing the response to auxin (Lee *et al.*, 2009). In *Capisicum annum*, overexpression of *CaGLIP1* has been shown to increase pathogen resistance, and resistance to abiotic stresses, including those induced by mannitol and drought (Hong *et al.,* 2008). Another *C. annum* GDSL enzyme, GDSL-lipase1 (CaGL1), is expressed upon induction of methyl jasmonic acid, which would be an expected response to stresses, but no associated physiological mechanism has been identified (Kim *et al.*, 2008).

Members of the GDSL superfamily have also been implicated in the development of plant organs, including floral organs and roots. In *A. thaliana* pollen, EXTRACELLULAR LIPASE 4 (EXL4) was found to regulate hydration, an essential step for pollination in species with dry stigmas (Updegraff *et al.*, 2009). However, the authors were unable to identify any differences in the accumulation of lipids or a specific mechanism that would account for changes in hydration. In another study of nectar proteins from *Jacaranda mimosifolia*, Jacaranda Nectar Protein (JNP1) was identified as a GDSL protein. The authors noted the presence of lipid bodies in the nectar, which were 5 μm in diameter or smaller (Kram *et al.,* 2008), which they suggested might be

involved in pollinator attraction or preventing microbial growth in the nectar. Finally, *Brassica napus* sinapoylcholine 3 (BnSCE3), another GDSL protein, was found to hydrolyze sinapine, an alkaloid often found in seeds of the *Brassicaceae* family, which promotes germination (Clauß *et al.*, 2008). In addition to sinapine, BnSCE3 has been found to catalyze the hydrolysis of many other choline molecules, suggesting a wide substrate specificity.

In addition to affecting flower development, GDSL enzymes have also been strongly implicated in the development of roots, both directly, and in the formation of secondary metabolites. Early nodulins 8 (ENOD8), a GDSL protein, was purified from root nodules in *Medicago sativa*, and was not able to catalyze the hydrolysis of longer chain aliphatic esters indicating a lack of lipase activity (Pringle and Dickstein 2004). The authors also noted protein sequence similarities to, EP4 another protein localized to the cell wall, and hypothesized that the substrate of ENOD8 may be an acetylated extracellular carbohydrate. Acetylajmalan esterase (AAE), a GDSL protein in *Rauvolfia serpentine* (L.) hypothesized to be involved in the formation of ajmaline class of alkaloids, was shown through heterologous expression in *Nicotiana benthamiana* to catalyze the deacetylation of the precursor, 17-O-acetylajmaline to the final product, ajmaline (Ruppert *et al.*, 2005).

The formation of the cell wall is another area in which the GDSL enzymes have been implicated. One example of a GDSL involved in cell wall modifications is α-fucosidase 1 (AtFXG1) from *A. thaliana*, when overexpressed in *Pichia pastoris,* α-L-fucosidase activity could be detected in

the culture medium (De la Torre *et al.*, 2002). Additionally, BRITTLE LEAF SHEATH1 (BS1) is a GDSL protein that catalyzes the deacetylation of the xylan backbone, which is crucial for the formation of the secondary cell wall. Extensive characterization of the enzyme indicated that it is localized to the Golgi apparatus, the site of the modification of cell wall monomers, and found that BS1 preferentially deacetylates xylan monomers (Zhang *et al.*, 2017).

Finally, some GDSL enzymes have been reported to be acetylcholinesterases (AChE), which catalyze the hydrolysis of acetylcholine, a neurotransmitter in animals. In mammals, hydrolysis occurs after acetylcholine releases from receptors and prevents a continuous electrical impulse (Kelly *et al.*, 1979). Although plants lack a nervous system, there have been reports of both acetylcholine and acetylcholinesterase in various plant species (Evans, 1972; Fluck and Jaffe, 1974).

Characterization of a putative acetylcholinesterase from *Zea mays*, indicated that it was able to hydrolyze acetylcholine, however the enzyme had weak hydrolytic activity (Yamamoto *et al.*, 2008). Subcellular localization following overexpression in *O. sativa* suggested that the AChE was localized to the cell wall and it was hypothesized to be involved in trafficking small molecules between cells (Yamamoto and Momonoki, 2008). However, there is some disagreement over whether or not GDSL enzymes truly possess AChE activity. Characterization of the *A. thaliana* ortholog revealed that the enzyme did not possess such an activity; however, the enzyme did have lipase activity, with a preference for long chain esters (Muralidharan *et al.*, 2013). Further

study of the roles of plant acetylcholinesterases and their substrates will be required to determine whether their functions are similar to homologs from animals.

Other plant GDSL enzymes have been identified and characterized to some degree but have yet to be assigned a physiological function. For example, lanatoside 15'-*O*-acetylesterase (LAE) from *Digitalis lanata* was purified from *in vitro* cultured cells which catalyzed ester hydrolysis (Kandzi *et al.*, 1997). As another example, black-grass (*Alopecurus myosuroides*), a weedy species, was found to have a GDSL protein, AmGDSH1, that differs slightly from most of the other GDSLs proteins as the canonical site is actually GDSF (Cummins and Edwards, 2004). No activity has been described for that protein.

In general, little is known about the function of the GDSL enzymes in plants and few have been characterized in plants thus far. The most revealing cases occur in situations where the native substrate can be identified together with the enzyme, potentially allowing mechanistic studies, but these cases are exceptionally rare.

GDSL Enzymes Involved in Cuticle Formation

For a long time, members of the GDSL superfamily were hypothesized to be involved in the formation of the plant cuticle. One member of the GDSL esterase/lipase superfamily was identified in *Agave americana*, named AgaSGNH, and shown to be present in the epidermis during rates of rapid leaf

elongation (Reina *et al.*, 2007). In *Arabidopsis thaliana*, co-silencing of two GDSL proteins resulted in severe floral organ fusion and a change in the ultrastructure of the epidemical cells, phenotypes which are typical in cuticle associated mutants (Shi *et al.*, 2011). A thorough analysis of the extracellular proteome in *Solanum lycopersicum* (tomato) identified two GDSL proteins as some of the most abundant in the collected samples (Yeats *et al.*, 2012).

In 2012, two studies identified the function of the GDSL enzyme that are abundant in the tomato fruit epidermis. The first of these studies characterized a mutant generated with the mutagen ethyl methansulfonate (EMS), *cutin deficient 1 (cd1)*, which was reported to exhibit a severe depletion of polymeric cutin (~95%) in the fruit cuticles but did accumulate the cutin monomer 2-mono(10,16-dihydroxyhexadecanoyl)glycerol (2-MHG). Incubating CD1 with 2-MHG resulted in a series of oligomers that were detected using matrix-assisted laser desorption ionization time of flight (MALDI-TOF) mass spectrometry (Yeats *et al.*¸ 2012). The other study used RNA interference (RNAi) to suppress expression of the same GDSL gene (termed GDSL1), which resulted in similar reduction in polymeric cutin as well as pores in the cutin matrix (Girard *et al.*, 2012). Further genetic analysis of homologs of CD1/GDSL1, resulted in the identification of several other GDSL genes, which were named as members of the cutin synthase-like (CUS) family, including an ortholog in *A. thaliana* which had previously been reported to enhance salt tolerance when overexpressed (Naranjo *et al.*, 2006). Furthermore, cutin synthase activity was exhibited by CUS proteins from *A. thaliana* and the moss

Physcomitrella patens (Yeats *et al.*, 2014), indicating a conserved mechanism for cutin formation in land plants.

In addition to the cutin synthases, there has been a report of a putative cutinase, an enzyme able to degrade the cutin matrix, which is also a member of the GDSL esterase/lipase superfamily (Takahashi *et al.*, 2010). This enzyme, CUTICLE DESTRUCTING FACTOR 1 (CDEF1), from *A. thaliana* was identified using an antibody raised against a fungal cutinase. In addition, ectopic expression, driven by the constitutive 35S promoter, resulted in both disruptions of the cuticle and areas where the cuticle was missing entirely. However, no abnormal phenotype was detected in a *cdef1* mutant which carried a T-DNA insertion in the coding region of *CDEF1* and no *in vitro* activity has been shown for the enzyme to this point.

Conclusions

There is still much to be learned about plant GDSL enzymes and their role in the formation of cutin. To date, few CUS proteins have been characterized, including the initial CUS protein identified, SLCUS1. Questions still remain about the degree to which paralogous members of the CUS protein family have overlapping functions in the formation of cutin. In the *slcus1* EMS lines, the fruits accumulated a thin layer of polymeric cutin, approximately 5% that of the wild type fruit (Yeats *et al.*, 2012), indicating that other enzymes polymerize cutin in tomato fuit. Moreover, electron microscopy has been used to identify a thin, electron dense layer on the exterior of tomato ovary,

epidermal cells which has been hypothesized to be the initial cuticle (Segado *et al.*, 2016). However, there have not been any mutations in cuticle-associated genes which result in abnormal ovary phenotypes, including *slcus1*. Nor were there any abnormal phenotypes identified in the flowers of *slcus1* as has been identified in mutants for cuticle-associated genes in *A. thaliana* (Shi *et al*., 2011). The goals of this study were three-fold; first, to determine whether SLCUS2 exhibits similar cutin synthase activity to SLCUS1, *in vitro*; second, to identify the SLCUS protein that contributes to the polymerization of cutin in tomato fruit; and third, to ascertain whether SLCUS2 is involved in the formation of cuticle in tomato flowers.

REFERENCES

Akoh, C.C., Lee, G.C., Liaw, Y.C., Huang, T.H. and Shaw, J.F. (2004) GDSL Family of Serine Esterases/Lipases. *Prog. Lipid Res.* **43**, 534-552.

Agee, A.E., Surpin, M., Sohn, E.J., Girke, T., Rosado, A., Kram, B.W., Carter, C., Wentzell, A.M., Kliebenstein, D.J., Jin, H.C., Park, O.K., Jin, H., Hicks, G.R. and Raikhel, N.V. (2010) MODIFIED VACUOLE PHENOTYPE1 is an Arabidopsis myrosinase-associated protein involved in endomembrane protein trafficking. *Plant Physiol.* **152**, 120-132.

CDBM. T MaBI (2008) The enzyme market survey. http://www.cbdmt.com/index/php?id=4. Accessed Oct 2018.

Chahinian, H., Nini, L., Boitard, E., Dubés, J.P., Comeau, L.C. and Sarda, L. (2002) Distinction between esterases and lipases: a kinetic study with vinyl esters and TAG. *Lipids.* **7**, 653-662.

Cheeseman, J.D., Tocilj, A., Park, S., Schrag, J.D. and Kazlauskas, R.J. (2004) Structure of an aryl esterase from Pseudomonas fluorescens. *Acta. Crystallogr. D.: Biol. Crystallogr*. **60**, 1237–1243.

Chepyshko, H., Lai, C.P., Huang, L.M., Liu, J.H. and Shaw, J.F. (2012) Multifunctionality and discovery of GDSL esterase/lipase gene family in rice (*Oryza sativa* L. *japonica)* genome: new insights from bioinformatics analysis. *BMC Genomics* **13**, 309.

Clauß, K., Baumert, A., Nimtz, M., Milkowski, C. and Strack, D. (2008) Role of a GDSL lipase-like protein as sinapine esterase in Brassicaceae. *Plant J.* **53**, 802-813.

Cummins, I. and Edwards, R. (2004) Purification and cloning of an esterase from the weed black-grass (*Alopecurus myosuroides*), which bioactivates aryloxyphenoxypropionate heribicides. *Plant J.* **39**, 894-904.

De la Torre, F., Sampedro, J., Zarra, I. and Revilla, G. (2002) AtFXG1, an Arabidopsis gene encoding α-L-fucosidase active against fucosylated xyloglucan oligosaccharides. *Plant Physiol.* **128**, 247-255.

Dong, X., Yi, H., Han, C.T., Nou, I.S. and Hur, Y. (2016) GDSL esterase/lipase genes in *Brassica rapa* L.: genome-wide identification and expression analysis. *Mol. Genet. Genom.* **291**, 531-542.

Evans, M.L. (1972) Promotion of cell elongation in *Avena coloepltiles* by acetylcholine. *Plant Physiol*. **50**, 414-416.

Fluck, R.A. and Jaffe, M.J. (1974) Cholinesterase from plant tissues. III. Distribution and subcellular localization in *Phaseolus aureus* Roxb. *Plant Physiol.* **53**, 752-758.

Freedonia. (2009) World Enzyme Market. Report Linker. http://www.reportlinker.com/p0148002/World-Enzymes-Market.html. Accessed Oct 2018.

Girard, A-L., Mounet, F., Lemaire-Chamley, M., Gaillard, C., Elmorjani, K., Vivancos, J., Runavot, J.L., Quemener, B., Petit, J., Germain, V.,

Rothan, C., Marion, D. and Bakan, B. (2012) Tomato GDSL1 is required for cutin deposition in the fruit cuticle. *Plant Cell* **24**, 3119-3134.

Hasan, F., Shah, A.A. and Hameed, A. (2005) Industrial applications of microbial lipases. *Enzyme Microb. Technol.* **39**, 235-251.

Houde, A., Kademi, A. and Leblanc D. (2003) Lipases and their industrial applications: an overview. *Appl. Biochem. Biotechnol.* **118**, 155-170.

Hong, J.K., Choi, H.W., Hwang, I.S., Kim, D.S., Kim, N.K., Choi, D.S., Kim, Y.J. and Hwang, B.K. (2008) Function of a novel GDSL-type pepper lipase gene, *CaGLIP1* in disease susceptibility and abiotic stress tolerance. *Planta* **227**, 539-558.

Huang, Y.T., Liaw, Y.C., Gorbatyuk, V.T. and Huang, T.H. (2001) Backbone dynamics of *Escherichia coli* thioesterase/protease I: Evidence of a flexible active-site environment for a serine protease. *J. Mol. Biol.* **307**, 1075-1090.

Ito, T., Kikuta, H., Nagamori, E., Honda, H., Ogino, H., Ishikawa, H. and Kobayashi T. (2001) Lipase production in two-step fed-batch culture of organic solvent-tolerant *Psuedomonas aeruginosa* LST-03. *J. Biosci. Bioeng.* **91**, 245-250.

Kandzia, R., Grimm, R., Eckerskorn, C., Lindemann, P. and Luckner, M. (1998) Purification and characterization of lanatoside 15’-O-acetylesterase from *Digitalis lanata* Ehrh. *Planta.* **204**, 383-389.

Kelly, R.B., Deutsch, J.W., Carlson, S.S. and Wagner J.A. (1979) Biochemistry of neurotransmitter release. *Annu. Rev. Neurosci.* **2,** 399-466.

Khan, F.I., Lan, D., Durrani, R., Huan, W., Zhao, Z. and Wang Y. (2017) The lid domain in lipases: structural and functional determinant of enzymatic properties. *Frontiers Bioeng. Biotechnol.* **5**, 1-13.

Kilcawley, K.N., Wilkinson, M.G. and Fox, P.F. (2005) A novel two-stage process for the production of enzyme-modified cheese. *Food Res. Int.* **39**, 619-627

Kim, K.J., Lim, J.H., Kim, J.H., Kim, M.J., Chung, H.M. and Paek, K.H. (2008) GDSL-lipase1 (CaGL1) contributes to wound stress resistance by modulation of CaPR-4 expression in hot pepper. *Biochem. Biophys. Res. Commun.* **374**, 693-698.

Kram, B.W., Bainbridge, E.A., Perera, M.A.D.N. and Carter C. (2008) Identification, cloning and clarification of a GDSL lipase secreted into the nectar of *Jarcaranda mimosifolia*. *Plant Mol. Biol.* **68**, 173-183.

Kwon, S.J., Jin, H.C., Lee, S., Nam, M.H., Chung, J.H., Kwon, S.I., Ryu, C.M. and Park, O.K. (2009) GDSL lipase-like 1 regulates systemic resistance associated with ethylene signaling in Arabidopsis. *Plant J.* **58**, 235-245.

Lai, C.P., Huang, L.M., Chen, L.F.O., Chan, M.T. and Shaw J.F. (2017) Genome-wide analysis of GDSL-type esterases/lipases in *Arabidopsis.* *Plant Mol. Biol.* **95**, 181-197.

Lee, D.S., Kim, B.K., Kwon, S.J., Jin, H.C. and Park, O.K. (2009) Arabidopsis GDSL lipase 2 plays a role in pathogen defense via negative regulation of auxin signaling. *Biochem. Biophys. Res. Commun.* **379**, 1038-1042.

Li, J., Derewenda, U., Dauter, Z., Smith, S. and Derewenda, Z.S. (2000) Crystal structure of the Escherichia coli thioesterase II, a homolog of the human Nef binding enzyme. *Nat. Struct. Biol.* **7**, 555–559.

Ling, H. (2008) Sequence analysis of GDSL lipase gene family in Arabidopsis thaliana. *Pak. J. Biol. Sci.* **11**, 763-767.

Lo, Y.C., Lee, Y.L., Shaw, J.F. and Liaw, Y.C. (2000) Crystallization and preliminary X-ray crystallographic analysis of thioesterase I from Escherichia coli. *Acta. Crystallogr. D.: Biol. Crystallogr.* **56**, 756–757.

Lo, Y.C., Lin, S.C., Shaw, J.F. and Liaw, Y.C. (2000) Crystal structure of Escherichia coli thioesterase I/protease I/lysophospholipase L1: consensus sequence blocks constitute the catalytic center of SGNH-hydrolases through a conserved hydrogen bond network. *J. Mol. Biol.* **330**, 539–551.

Mathews, I., Soltis, M., Saldajeno, M., Ganshaw, G., Sala, R., Weyler, W., Cervin, M.A., Whited, G. and Bott, R. (2010) Structure of a Novel Enzyme That Catalyzes Acyl Transfer to Alcohols in Aqueous Conditions. *Biochemistry* **46**, 8969–8979.

Muralidharan, M., Buss, K., Larrimore, K.E., Segerson, N.A., Kannan, L. and Mor, T.S. (2013) The *Arabidopsis thaliana* ortholog of a purported

maize cholinesterase gene encodes a GDSL-lipase. *Plant Mol. Biol.* **81**, 565-576.

Naranjo, M.A., Forment, J., Roldan, M., Serrano, R. and Vicente, O. (2006) Overexpression of *Arabidopsis thaliana LTL1,* a salt-induced gene encoding a GDSL-motif lipase, increases salt tolerance in yeast and transgenic plants. *Plant, Cell Environ.* **29**, 1890-1900.

Oh, I.S., Park, A.R., Bae, M.S., Kwon, S.J., Kim, Y.S., Lee, J.E., Kang, N.Y., Lee, S., Cheong, H. and Park, O.K. (2005) Secretome analysis reveals an *Arabidopsis* lipase involved in defense against *Alternaria brassicicola*. *Plant Cell* **17**, 2832-2847.

Ouyang, S., Zhu, W., Hamilton, J., Lin, H., Campbell, M., Childs, K., Thibaud-Nissen, F., Malek, R.L., Lee, Y., Zheng, L., Oris, J., Haas, B., Wortman, J. and Buell, C.R. (2007) The TIGR Rice Genome Annotation Resource: improvements and new features. *Nucleic Acids Res.* **35**, D883-D887.

Pandey, A., Benjamin, S., Soccol, C.R., Nigam, P., Krieger, N. and Soccol, V.T. (1999) The realm of microbial lipases in biotechnology. *Biotechnol. Appl. Biochem.* **29**, 119-131.

Peterson, E.I., Valinger, G., Solkner, B., Stubenrauch, G. and Schwab, H. (2001) A novel esterase from *Burkholderia gladioli* which shows high deacetylation activity on Cephalosprins is related to β-lactomases and DD-peptidases. *J. Biotechnol.* **89**, 11-25.

Pleiss, J., Fischer, M., Peiker, M., Thiele, C. and Schmid, R.D. (2000) Lipase engineering database: Understanding and exploiting sequence-structure-function relationships. *J Mol Catal B: Enzym* **10**, 491-508.

Pringle, D. and Dickstein, R. (2004) Purification of ENOD8 proteins from Medicago sativa root nodules and their characterization as esterases. *Plant Physiol. Biochem.* **42**, 73-79.

Reina, J.J., Guerroro, C. and Heredia, A. (2007) Isolation, characterization, and localization of *AgaSGNH* cDNA: a new SGNH-motif plant hydrolase specific to *Agave Americana* L. leaf epidermis. *J. Exp. Bot.* **58**, 2717-2731.

Ruppert, M., Woll, J., Giritch, A., Genady, E., Ma, X. and Stöckigt, J. (2005) Functional expression of an ajmaline pathway-specific esterase from *Rauvolfia* in a novel plant-virus expression system. *Planta* **222**, 888-898.

Shi, J.X., Malitsky, S., De Oliveira, S., Branigan, C., Franke, R.B., Schreiber, L. and Aharoni, A. (2011) SHINE transcription factors act redundantly to pattern the archetypal surface of Arabidopsis flower organs. *PLoS Genet.* **7**, e1001388.

Svendsen, A. (2000) Lipase protein engineering. *Biochem Biophys Acta.* **1543**, 223-238.

Takahashi, K., Shimada, T., Kondo, M., Tamai, A., Mori, M., Nishimura, M. and Hara-Nishimura, I. (2010) Ectopic expression of an esterase,

which is a candidate for the unidentified plant cutinase, causes cuticular defects in *Arabidopsis thaliana*. *Plant Cell Physiol.* **51**, 123-131.

Updegraff, E.P., Zhao, F. and Preuss, D. (2009) The extracellular lipase EXL4 is required for efficient hydration of *Arabidopsis* pollen. *Sex Plant Reprod.* **22**, 197-204.

Upton, C. and Buckley, J.T. (1995) A new family of lipolytic enzymes? *Trends Biochem. Sci.* **20**, 178-179.

van den Berg, B. (2010) Crystal structure of a full-length autotransporter. *J. Mol. Biol.* **396**, 627–633.

Verger, R. (1997) 'Interfacial activation' of lipases: facts and artifacts. *Trends Biotechnol.* **15**, 32-38.

Volokita, M., Rosilio-Brami, T., Rivkin, N. and Zik, M. (2010) Combining comparative sequence and genomic data to ascertain phylogenetic relationships and explore the evolution of the large GDSL-lipase family in land plants. *Mol. Biol. Evol.* **28**, 551-565.

Wei, Y., Schottel, J.L., Derewenda, U., Swenson, L., Patkar, S., Derewanda, Z.S. (1995) A novel variant of the catalytic triad in the *Streptomyces scabies* esterase. *Nat. Struct. Mol. Biol.* **3**, 218-223.

Yamamoto, K. and Momonoki, Y.S. (2008) Subcellular localization of overexpressed maize AChE gene in rice plant. *Plant Signaling and Behav*. **8**, 576-577.

Yamamoto, K., Oguri, S. and Momonoki, Y.S. (2008) Characterization of trimeric acetylcholinesterase from a legume plant, *Macroptilum atropupureum* Urb. *Planta* **227**, 809-822.

Yeats, T.H., Howe, K.J., Matas, A.J., Buda, G.J., Thannhauser, T.W. and Rose, J.K.C. (2010) Mining the surface proteome of tomato (*Solanum lycopersicum*) fruit for proteins associated with cuticle biogenesis. *J. Exp. Bot.* **61**, 3759-3771.

Yeats, T.H., Huang, W., Chatterjee, S., Viart, H.M.F., Clausen, M.H., Stark, R. E. and Rose, J.K.C. (2014) Tomato Cutin Deficient 1 (CD1) and putative orthologs comprise an ancient family of cutin synthase-like (CUS) proteins that are conserved among land plants. *Plant J.* **77**, 667–75

Yeats, T.H., Martin, L.B.B., Viart, H.M.F., Isaacson, T., He, Y., Zhao, L., Matas, A.J., Buda, G.J., Domozych, D.S., Clusen, M.H. and Rose, J.K.C. (2012) The identification of cutin synthase: formation of the plant polyester cutin. *Nat. Chem. Biol.* **8**, 609-611.

Youens-Clark, K., Buckler, E., Casstevens, T., Chen, C., Dederck, G., Derwent, P., Dharmawardhana, P., Jaiswal, P., Kersey, P., Karthikeyan, A.S., Lu, J., McCouch, S.R., Ren, L., Spooner, W., Stein, J.C., Thomason, J., Wei, S. and Ware, D. (2010) Gramene database in 2010: updates and extensions. *Nucleic Acids Res.* **39**, D1085-D1094.

Zhang, B., Zhang, L., Li, F., Zhang, D., Liu, X., Wang, H., Xu, Z., Chu, C. and Zhou, Y. (2017) Control of secondary cell wall patterning involves xylan deacetylation by a GDSL esterase. *Nat. Plants* **3**, DOI:10.1038.

Zhang, Z., Ober, J.A. and Kliebenstein D.J. (2006) The gene controlling the quantitative trait locus EPITHIOSPECIFIER MODIFIER1 alters glucosinolate hydrolysis and insect resistance in *Arabidopsis. Plant Cell* **18**, 1524-1536.

CHAPTER 2

Biochemical and physiological characterization of CUS2, an ortholog of a tomato cutin synthase

Introduction

The plant cuticle coats the outer surfaces of almost all land plants, with the exception of the stems of woody plants, and likely evolved as a mechanism for limiting transpirational water loss (Fich *et al.*, 2016; Yeats *et al*., 2013). The cuticle consists of two primary components: a range of predominantly aliphatic, easily-soluble hydrocarbons, collectively referred to as waxes, and an insoluble polyester, cutin, which is composed primarily of polyhydroxylated fatty acids and di-acids (Samuels *et al.*, 2008; Edwards *et al.*, 1996). Though many of the functions of the cuticle have been associated with waxes (Schreiber, 2010), cutin is the predominant component of the mass of the cuticle (Baker *et al.*, 1982), and contributes to the viscoelasticity of the cuticle and defines organ boundaries during organogenesis (Tsubaki *et al.*, 2012; Krolikowski *et al.*, 2003).

The cutin monomer composition can vary between species, and even organs in a single species; however, the cutin monomers are typically long chain (typically C16 or C18) fatty acids containing an ω-hydroxyl group, and sometimes a mid-chain hydroxyl or other functional group (Holloway, 1982). In contrast to the sometimes extensive monomer composition of many plant cuticles, little is known about cutin polymer structure, and much of our understanding has resulted from partial depolymerization of isolated cuticles

and analysis of the degradation products (Fich *et al.*, 2016). Such studies suggest that both ω- and mid-chain hydroxyls are incorporated into the polymer structure resulting a highly branched polymer (Kolattukudy, 1977; Deas and Holloway, 1977).

Until recently, the mechanism of cutin polymerization has been poorly understood. The first enzyme identified as being involved in the polymerization of cutin was discovered in tomato (*Solanum lycopersicum*) through two, independent mutant lines that accumulated both less polymeric cutin but also accumulated the soluble glyceryl ester of the cutin monomer 2-mono(10,16-dihydroxyhexadecanoyl)glycerol (2-MHG) (Yeats *et al.*, 2012; Girard *et al.*, 2012). This phenotype was caused by a mutation in a member of the GDSL-esterase/lipase superfamily, a protein encoded by *CUTIN DEFICIENT1* (*CD1*, Solyc11g006250).

CD1 catalyzes the polymerization of cutin oligomers through successive rounds of transesterification of 2-MHG. Briefly, CD1 reacts with a molecule of 2-MHG, forming an acyl-enzyme intermediate and releasing free glycerol. Subsequently, the acyl-enzyme intermediate interacts with a second molecule of 2-MHG, transferring a molecule of 10,16 dihydroxyhexadecanoic acid (DHHA), initiating the formation of cutin oligomers. Subsequent genetic analysis of GDSLs was performed and a small subclade of GDSLs was identified throughout a range of land plants (Yeats *et al.*, 2014). Members of this subclade were named the Cutin Synthase-like (CUS) proteins and CD1 was thus renamed SLCUS1. Catalysis of 2-MHG transesterification was

shown to be conserved in the CUS protein subclade, with activity demonstrated not only for SLCUS1, but also homologs from *Arabidopsis thaliana* and the moss, *Physcomitrella patens* (Yeats *et al.*, 2014).

In addition to SLCUS1, four other CUS genes were identified in tomato: *SLCUS2*, Solyc04g050730; *SLCUS3*, Solyc04g050570; *SLCUS4*, Solyc06g083650; and *SLCUS5*, Solyc0906360. To date, little has been reported about the degree to which CUS paralogs have an overlapping role in cutin polymerization, although there is evidence of some overlap in *A. thaliana*. The use of artificial microRNA that suppressed the expression of two homologs of CUS1, At5g33370 (*AtCUS2*) and At3g04290 (*AtCUS1*), resulted in abnormal phenotypes commonly described in mutants with abnormal cuticles: the flower petals fused and lacked cuticular nanoridges on the abaxial surfaces (Shi *et al.*, 2011). It was also reported that loss of function of *A. thaliana AtCUS2* is sufficient to disrupt the formation of nanoridges in the cuticle of the sepal but has only moderate effects on petal development (Hong *et al.*, 2017).

Other than these studies in *A. thaliana*, little is known about CUS enzyme function an potential overlapping roles. Despite a null mutation that removes two of the three catalytic residues, a small amount of polymeric cutin is present in fruit from the *slcus1* line, accounting for approximately 5% of the polymeric cutin levels that are typical in wild type plants (Yeats *et al.,* 2012). Two explanations for the residual polymeric cutin in *slcus1* fruits are that this is a result of a compensatory CUS protein, or that there is a secondary

mechanism by which the polymer is formed. In addition, the tomato ovary have a thin electron dense layer even at the initiation of fruit development, which has been hypothesized to be the initial stages of the cuticle (Segado *et al.*, 2016). However, no source for the deposition of the cuticle at this stage of development has been reported. Given the role of a functional cuticle in defining organ boundaries, it is likely that a SLCUS protein is responsible for polymerizing the residual cutin in *slcus1* fruit and may be involved in the formation of cutin in the initial stages of fruit development. The goals of this study were three-fold; first, to determine whether SLCUS2 exhibits similar cutin synthase activity to SLCUS1, *in vitro*; second, to identify the SLCUS protein that contributes to the polymerization of cutin in tomato fruit; and third, to ascertain whether SLCUS2 is involved in the formation of cuticle in tomato flowers.

Results

SLCUS2 is the most abundantly expressed *SLCUS* in the fruit

The Tomato Expression Atlas < http://tea.sgn.cornell.edu> was used to identify potential CUS genes involved in the formation of cutin in the fruit as this dataset offers expression throughout fruit development and specific tissue in the pericarp (Shinozaki *et al.*, 2018). Expression data from both the outer epidermis and inner epidermis of the fruit were examined as many cuticle-associated genes are expressed in both (Matas *et al.*, 2011), although to date disrupted inner epidermal cuticles and related phenotypes have not been

reported for cuticle-associated mutants. Notably, the expression of *SLCUS1* was found to be higher than that the other CUS genes regardless of fruit tissue or developmental stage. Of the four remaining CUS genes, *SLCUS2* was the second most highly expressed in both the inner and outer epidermis (Figure 2.1a). *SLCUS2* was therefore considered as a likely candidate for the synthesis of the cutin polymer in tomato fruit.

SLCUS1 and SLCUS2 share 75% amino acid sequence identity and 89% sequence similarity. No protein structure for any CUS protein been solved to date and so the protein threading software PHYRE2 <www.sbg.ic.ac.uk/~phyre2/html/page.cgi?id=index> was used to generate models based on solved protein structures of the most closely related homologs using the “normal” procedure (Kelley *et al.*, 2015). This follows four steps which include generating a hidden Markov model (HMM) through multiple sequence alignment and secondary structure prediction, scanning against a database of HMMs of proteins of known protein structures to form a crude backbone, modelling loops into the crude backbone to account for insertions and deletions of amino acids, and finally, placing amino acid side chains to generate the completed model. Both SLCUS1 and SLCUS2 models were generated using the crystal structure of EstA, an autotransporter from *Pseudomonas aeruginosa* (PDB no. c3kvnA) with 88% coverage, 100% confidence, and 22% ID.

A characteristic of members of the GDSL esterase/lipase superfamily is the presence of five highly conserved amino acid blocks (Upton and Buckley,

1995). Four of these contain residues that make up the catalytic triad and oxyanion hole, and all play important roles in the catalytic activity of the enzyme (Akoh *et al.*, 2004). The highly conserved amino acid blocks were labelled as I, II, III, and IV and the conserved domains in SLCUS1 and SLCUS2 were highlighted as follows: GDSL conserved blocks (blue), catalytic triad (red), and oxyanion hole (green) (Figure 2.1b). The close proximity of these residues in the predicted structures provides some confidence that they indeed serve as the active site of catalysis it the two CUS proteins and that the overall function of the two proteins is likely to be similar (Figure 2.1c).

Characterization of SLCUS2 Activity

To investigate whether SLCUS2 has cutin synthase activity, it was expressed in *Nicotiana benthamiana* leaves with a C- terminal His-tag and purified using nickel-column affinity purification and size exclusion chromatography. SLCUS1 had an expected size of 41 kDa and SLCUS2 had an expected size of 43 kDa (Figure 2.2). The purified recombinant protein was then incubated with 2-MHG and analyzed using matrix-assisted laser desorption/ionization (MALDI-TOF) mass spectrometry, as previously described (Yeats *et al.*, 2012). SLCUS1, purified from *Nicotiana benthamiana* leaves as previously described (Yeats *et al.*, 2012) and SLCUS2 were individually incubated with 2-MHG as previously described (Yeats *et al.*, 2014) (Figure 2.3). In addition to incubating the enzymes, enzymes which had been denatured by boiling were incubated with 2-MHG as a negative control and

samples containing DMSO instead of 2-MHG were analyzed using MALDI-TOF as a background control which was subtracted from the experimental spectra.

In both individual incubations, a series of peaks corresponding to the cutin oligomers were identified in the MALDI-TOF spectra, as well as DHHA, the hydrolysis product of 2-MHG. For both enzymes, oligomers could be detected up to n=10, where n is the number of DHHA molecules in the oligomer. To better understand whether the two enzymes perform distinct reactions, equal amounts (0.25 ug) of SLCUS1 and SLCUS2 were co-incubated with 2-MHG. Co-incubation with both SLCUS1 and SLCUS2 had no effect on the overall oligomeric profile of the products (Figure 2.3). Parameters were tested including initially incubating 2-MHG with one enzyme and then adding the other after the reaction had begun or by altering the amount of either enzyme during coincubation (Figure 2.4). However, no differences in the spectra were observed.

Kinetic properties of SLCUS2

A previous report characterizing the enzymatic properties of SLCUS1 described a method for calculating the apparent Michaelis-Menten kinetics, using a free glycerol assay (Yeats *et al.*, 2014). There are limitations when using this method because of the nature of the reaction: measurement of Michaelis-Menten kinetics is reliant on saturating the enzyme with the substrate in the initial step of the reaction. However, because the SLCUS

enzymes use 2-MHG as both substrates, the K_m and k_{cat} can prove challenging to calculate. However, a similar approach was taken for recombinant SLCUS2 as was performed with SLCUS1 and the data were fitted to a Michaelis-Menten curve that indicated with an apparent K_m of 237 +/- 62 μM and an apparent k_{cat} of 0.198 +/- 0.013 s^{-1} (Figure 2.5, Table 2.1).

SLCUS2 **is expressed during early stages of fruit development and in floral tissue**

Analysis of expression data of SLCUS genes derived from the Tomato Expression Atlas (http://tea.sgn.cornell.edu/index) indicted that *SLCUS1* is expressed more abundantly than *SLCUS2* regardless of the developmental stage, and slightly later than *SLCUS2*. To further elucidate the expression of the two genes, quantitative PCR (qPCR) was used to determine expression over a time period of 5 days post anthesis (DPA) to 25 DPA, as well as the mature green (MG) and red ripe (RR) stages of development (Figure 2.6). This analysis confirmed that *SLCUS1* is more abundantly expressed than *SLCUS2* regardless of the developmental stage. However, there are clear differences in the expression patterns of the two genes. *SLCUS2* is expressed in earlier stages of fruit development. *SLCUS2* expression peaks at 10 DPA and by 20 DPA is barely detectable. *SLCUS1*, on the other hand, is expressed mostly at 15 and 20 DPA and becomes almost undetectable at the mature green stage.

The rate of fruit growth was measured to investigate a potential correlation between the expression patterns of the two CUS genes and the

rate of fruit expansion and cuticle deposition during development (Figure 2.7). Based on 15 replicates, the highest rate of growth was between five and ten DPA, after which time growth slowed. This corresponded to the point at which expression of *SLCUS2* was no longer detected.

Cuticle formation is also important for flower formation and characteristic fusion phenotypes have been identified in the flowers of *Arabidopsis thaliana* cuticle-associated mutants. Electron microscopy of tomato ovaries reveals a thin, electron dense layer, even at anthesis. This thin layer has been hypothesized to be the initial cuticle (Segado *et al.*, 2016).

To determine whether SLCUS2 catalyzes the polymerization of ovarian cutin, qPCR was used to analyze the expression of *SLCUS2* over floral development was measured using partially dissected flower. Prior to RNA extraction, ovaries were separated from the sepals, anthers, and petals (Figure 2.8). While there was *SLCUS2* expression detected in the ovary in flowers between 8 and 9 mm, higher levels of *SLCUS2* was detected in the non-ovarian tissue at that stage. To further elucidate the tissue in which *SLCUS2* was expressed, flowers from the same stage (8-9 mm) were fully dissected into the ovary, petals, sepals, and anthers and qPCR was used to analyze the expression of the gene (Figure 2.9). The majority of *SLCUS2* expressed was found to be in the petals and the sepals.

Generating *slcus2* null mutants using CRISPR/Cas9

To investigate the biological significance of SLCUS2 knockout lines were generated using CRISPR/Cas9 vectors that included two single guide RNAs (sgRNAs) as previously described (Brooks *et al*, 2014) within the *SLCUS2* coding region and transformed into the M82 cultivar. To identify lines which carried mutations that would disrupt the function of SLCUS2, PCR was performed on ten T0 lines using primers that flanked the sgRNA targets. Of the ten T0 lines, only one of the transformants was possessed a mutation. This mutation resulted in a four-nucleotide deletion resulting in a premature stop codon, and a truncated SLCUS2 which lacked two residues of the catalytic triad. The resulting predicted protein lacked two residues of the catalytic triad as well as two residues that make up the oxyanion hole, a non-functional protein (Figure 2.10). Furthermore, qPCR was used to evaluate *SLCUS2* transcript levels, and only residual expression was detected in the fruit or the flowers of the KO plant during developmental periods that correspond to peak *SLCUS2* expression in wild type (Figure 2.11).

Analysis of fruit and flower cuticles in *slcus2*

To identify any abnormal phenotypes in the fruit and floral cuticle of the *slcus2* lines, two independent methods were chosen, measuring cuticle thickness following staining with a lipid stain, Oil Red O, and biochemical analysis using gas chromatography with flame ionization detector (GC-FID). For analysis of abnormal phenotypes in the fruits, two stages of fruit development were the focus of this study: 15 DPA and mature green. The

former was selected because it is the stage after *SLCUS2* expression has begun to decrease, allowing time for the enzyme to perform its function and the latter was selected as the stage at which the total cutin amount no longer changes (Baker *et al*, 1982). In the flowers, the petals were the focus of this study because it was the tissue in which *SLCUS2* was most highly expressed.

To characterize changes in the cuticle of *slcus2* fruits, cryosections were prepared from isolated fruit pericarps, treated with Oil Red O, and observed using differential interface contrast (DIC) light microscopy (Figure 2.12). While a decrease in cuticle thickness was clear in the mature green sl*cus1* fruit, there was no apparent difference between the WT and *cus2* lines. Quantitative differences in the cuticle of the three genotypes were made by measuring the cuticle thickness above each epidermal cell (Figure 2.13).

To determine compositional differences in the cutin monomers of the three genotypes, the cuticles of mature green fruits were enzymatically treated to remove polysaccharides, solvents to remove any waxes, and finally depolymerized through methanolysis. The resulting cutin monomers were then quantified using gas chromatography with a flame ionization detector (GC-FID) (Figure 2.14). While no differences were detected between the cutin monomer composition of *slcus2* and wild type fruits, there were statically significant differences between the two aforementioned genotypes and the cutin monomers from *slcus1* fruits.

Initial attempts to characterize flower petals using DIC light microscopy proved too difficult as the tissue proved too fragile to embed for

cyrosectioning. Instead, scanning electron microscopy (SEM) and transmission electron microscopy (TEM) were used to analyze structural features of the petal cuticle of *cus2* and M82 (Figure 2.15). However, no differences were observed between the wild type and *cus2* lines. While it has not been described in tomato flowers, a common phenotype associated with cuticle mutants is a change in the architecture of petal epidermal cells, as is the case in *A. thaliana* (Shi *et al.*, 2011). However, no such changes to epidermal cell morphology could be identified in the petals of *slcus2* (Figure 2.15 B, D) when compared to petals from M82 (Figure 2.15 A, C). In addition, TEM imaging did not identify any changes to the ultrastructure of cuticles from *slcus2* petals compared to the M82 petals (Figure 2.15 E, F). Total cutin composition was quantified using GC-FID of isolated petal cuticles and no significant differences were observed between the total cutin monomer levels of *slcus2* and M82 (Figure 2.16).

Discussion

While the mode of SLCUS1 action has been determined, there are still many questions about the basis of cutin synthesis and structure in tomato fruit. One central question is the basis of the residual cutin synthesis in the *slcus1* mutant. Here, the hypothesis was tested that SLCUS2 is responsible for that minor portion of cutin biosynthesis. This idea was supported by expression data indicating that it is the only other SLCUS gene expressed during tomato fruit development (Figure 2.1a). *SLCUS2* expression patterns were confirmed

with a more extensive expression analysis (Figure 2.6) which revealed that SLCUS2 is expressed earlier in fruit development than *SLCUS1*, albeit at much lower levels than *SLCUS1*.

Notably, the period of peak expression of *SLCUS2* corresponded to the period of the most rapid fruit expansion (Figure 2.7). It has been suggested that the growth of plant organs, including fruit, is limited by the epidermal cell layer, which is always under tension and constrains the growth of underlying tissue (Kutschera and Niklas, 2007). In addition to the epidermal cells, the cuticle is a covalently linked to the underlying epidermal cells, it is also under tension, as evidenced by the fact that isolated cuticle contracts while the tissue below the epidermis expands (Domínguez *et al.*, 2010). While isolated cutin has been shown to contribute little to the overall strength of the cuticle, it does contribute to the plasticity, allowing the cuticle to stretch under the tension of the expanding tissue (López-Casado *et al.*, 2007). To accommodate the expansion that the fruit undergoes, cutin must be synthesized and deposited in the cuticle, and the total amount of cutin increases during fruit development (Isaacson *et al.*, 2009). The expression of *SLCUS2* at the stages of development when the fruit is undergoing the most rapid increases in surface area is consistent with it contributing to the maintenance of cuticle deposition during fruit expansion.

Characterization of *SLCUS2* expression in flowers also indicated that it is expressed in petals, sepals and, to a lesser extent, ovaries (Figure 2.9). It has previously been reported that of cuticle-associated genes in *A. thaliana*,

including those of the cutin synthase homologs, are expressed in floral organs (Shi *et al.*, 2011; Hong *et al.,* 2016). Given the expression patterns of *SLCUS2*, it seems likely that encoded enzyme is responsible for the residual polymeric cutin in the *slcus1* fruits, which would account for approximately 5% of the total cutin. Although no abnormal phenotypes were observed in flowers of the *slcus1* lines, the expression data suggest that SLCUS2 is also involved in the polymerization of floral cutin. Whether or not the enzyme is also responsible for the polymerization of cutin in other organs (i.e. stems, leaves, etc.), or whether other *SLCUS* genes are involved in the formation of floral cutin was not tested and would require further study.

SLCUS2 was shown to catalyze cutin polymerization *in vitro* (Figure 2.3). It remains to be seen whether the two enzymes are responsible for the formation of entirely linear cutin oligomers, as is the case with SLCUS1, or whether the products of the two enzymes differ. In addition, a variety of co-incubation conditions were tested to determine whether the oligomeric profile would be affected. These trials included altering the relative amounts of SLCUS1 or SLCUS2 I the reaction, as well allowing the polymerization reaction to occur with one enzyme for a period of time before the addition of the other. Regardless of the conditions tested, no differences were detected. The Michaelis-Menten kinetics of SlCUS2 were determined as previously reported. While these numbers represent the *in vitro* polymerization reactions, the K_m values for the two enzymes were similar, though the K_m value for the SLCUS1 reaction was smaller than previously reported: 294 ± 24 μM

compared to 925 ± 98 μM (Yeats *et al.*, 2014). The reason for this change may be that the values reported in the Yeats et al. (2014) study reflected the activities of enzymes that had been flash frozen, which may affect the initial rate of the reaction. The k_{cat}, or amount of substrate an enzyme can convert into product per second, for SLCUS2 was much lower than that of SLCUS1, 0.198 ± 0.013 s^{-1} for SLCUS2 compared to 0.375 ± 0.008 s^{-1} for SLCUS1. This may suggest that SLCUS1 is able to polymerize cutin more quickly than SLCUS2; however, as previously mentioned, the measurement of CUS enzyme kinetics is complicated by the nature of the reaction.

Analysis of *SLCUS2* expression and *in vitro* activity provide evidence that it is involved in the synthesis of a portion of the total polymeric cutin in fruit as well as in flowers, particularly the petals. However, despite extensive characterization of the *cus2* lines, no discernable abnormal phenotype was detected. One possible explanation for this is that *SLCUS1* is consistently expressed at higher levels than *SLCUS2*, regardless of the developmental stage. At 10 DPA, the peak expression of *SLCUS2*, the expression of *SLCUS1* is ten-fold that of *SLCUS2*. Due to the differences in expression levels, the overall contribution of SLCUS2 to the total cutin amount of the fruit may be indistinguishable in the presence of *SLCUS1.*

Another possibility is that SLCUS2 contribute to polymeric cutin architecture in a way that is not distinguishable with the techniques used in this current study. Evidence has been presented that the cutin polymer in tomato is a highly branched (Deshmukh *et al.*, 2003). In one report, NMR

analysis of the SLCUS1 products indicated that the enzyme generates linear polymers *in vitro* (Yeats *et al.*, 2014). However, in another study, labeling of free hydroxyls of cutin extracted from fruit that had suppressed *SLCUS1* expression, revealed an increase in free mid-chain hydroxyl groups but not ω-hydroxyls (Girard *et al.*, 2015). It may that the effects of SLCUS2 action might be more easily determined using analytical tools, such as NMR, that can reveal more complex aspects of cutin polymer structure, tools

The GDSL esterase/lipase superfamily have gone through numerous duplication events (Chepyshko *et al.*, 2012). Based on the expression patterns of *SLCUS1* and *SLCUS2,* it is likely that both enzymes are involved in the deposition of polymeric cutin in the fruit. I propose that *SLCUS2* is an ancestral gene that is responsible for the deposition of basal amounts of polymeric cutin in fruit, as well as other organs, while *SLCUS1* resulted from a duplication event and controls the formation of most of the fruit cutin. Consistent with this idea, there is an almost 95% reduction in polymeric cutin in *slcus1* fruit, but the residual amount is more similar in levels to the cutin present on other tomato organs.

To address these possibilities, the EMS mutant of *slcus1* could be crossed with the *slcus2* generated through transformation with CRISPR/Cas9. Double mutants in the F2 lines would then be characterized as described above. To address architectural changes in the cutin polymer of *slcus1* and *slcus2,* techniques such as NMR and Fourier-transform infrared spectroscopy (FT-IR) might be used identify architectural changes that could not be detected

through microscopy or monomer composition analysis (Deshmukh *et al.*, 2003; Girard *et al*., 2015).

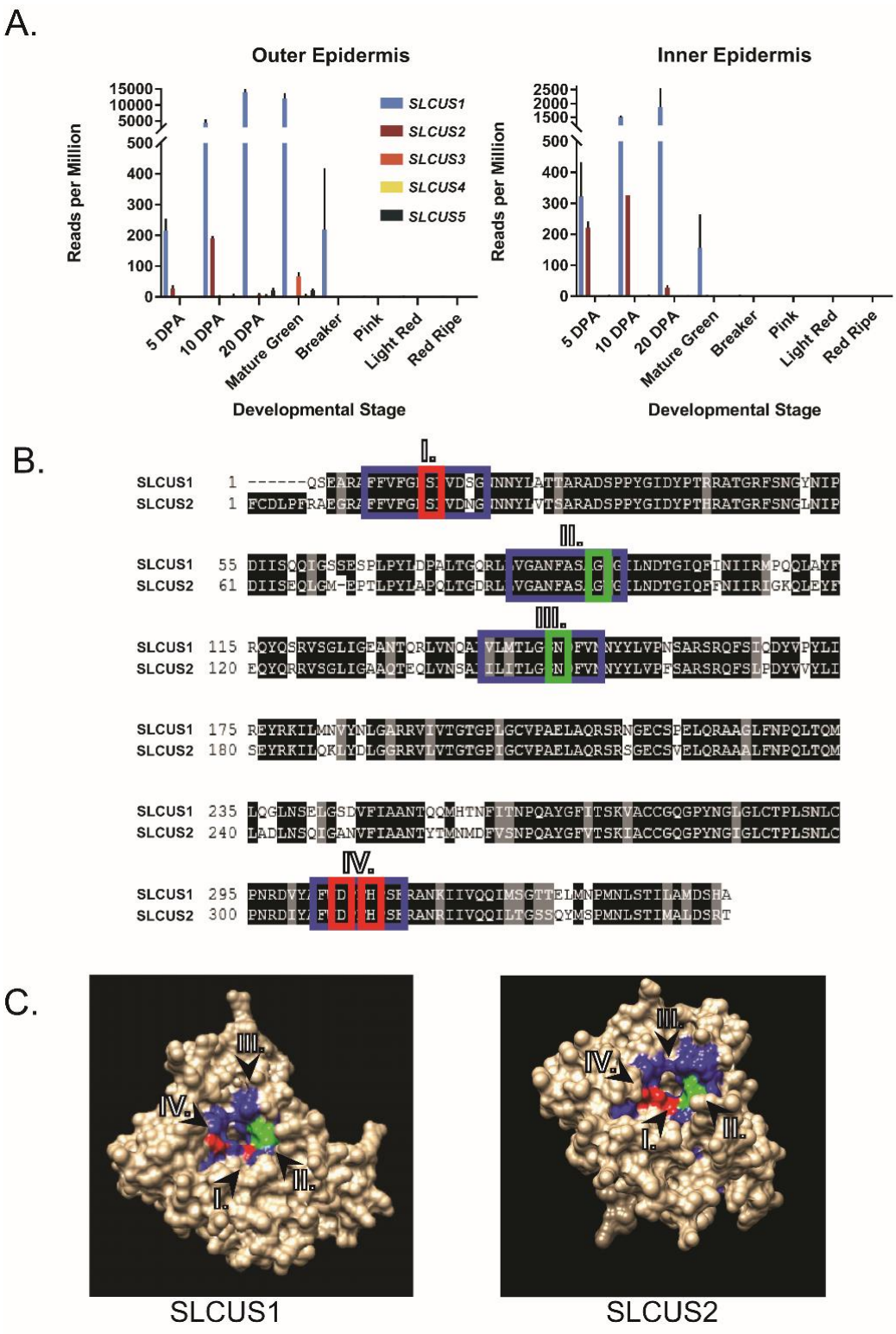

Figure 2.1 *SlCUS2* is expressed during fruit development and has a similar to SLCUS1 in amino acid sequence. (a) The expression of

SLCUS1 and *SLCUS2* as determined by the Tomato Expression Atlas (http://tea.sgn.cornell.edu). Expression is reported as Reads Per Million (RPM). DPA = days post anthesis. (b) Amino acid sequence alignment of SLCUS1 and SLCUS2. The alignment was preformed using T-coffee (http://tcoffee.crg.cat/) after removing the predicted N-terminal secretory signal peptides. Sequences highlighted in black indicate conserved amino acids, while those in dark grey indicate amino acid sequence similarity. Roman numerals I-IV represent amino acid blocks conserved in GDSL esterase/lipases Blue boxes indicate residues that are highly conserved in GDSL esterase/lipases, red boxes indicate residues in the catalytic triad, and green boxes indicate residues that form the oxyanion hole. (c) Hypothetical protein models of SLCUS1 and SLCUS2 as predicted by PHYRE2. Residues that are highly conserved or participate in catalytic function are highlighted and colored as indicated in section (b).

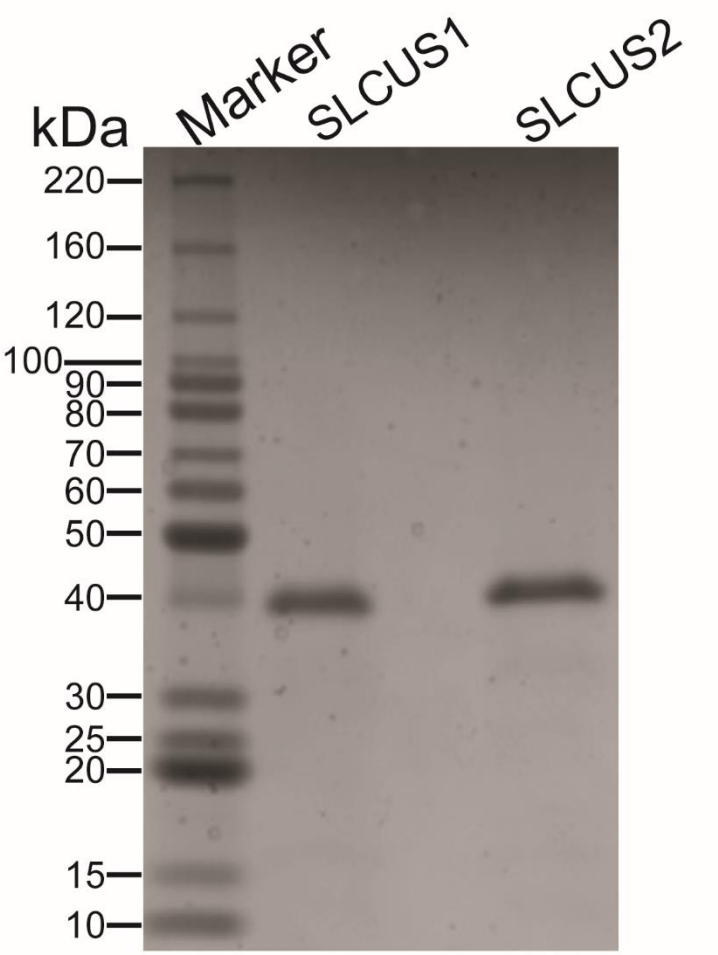

Figure 2.2 Purification of recombinant SLCUS1 and SLCUS2. SDS-PAGE gel showing 500 ng of recombinant SLCUS1 and SLCUS2, each with a C-terminal His-tag. The recombinant proteins were purified from *Nicotiana benthamiana* leaves by sequential nickel affinity chromatography and size exclusion chromatography and visualized using Coomassie stain. Protein ladder on gel is Invitrogen BenchMark^{TM} Protein Ladder (cat #10747-012).

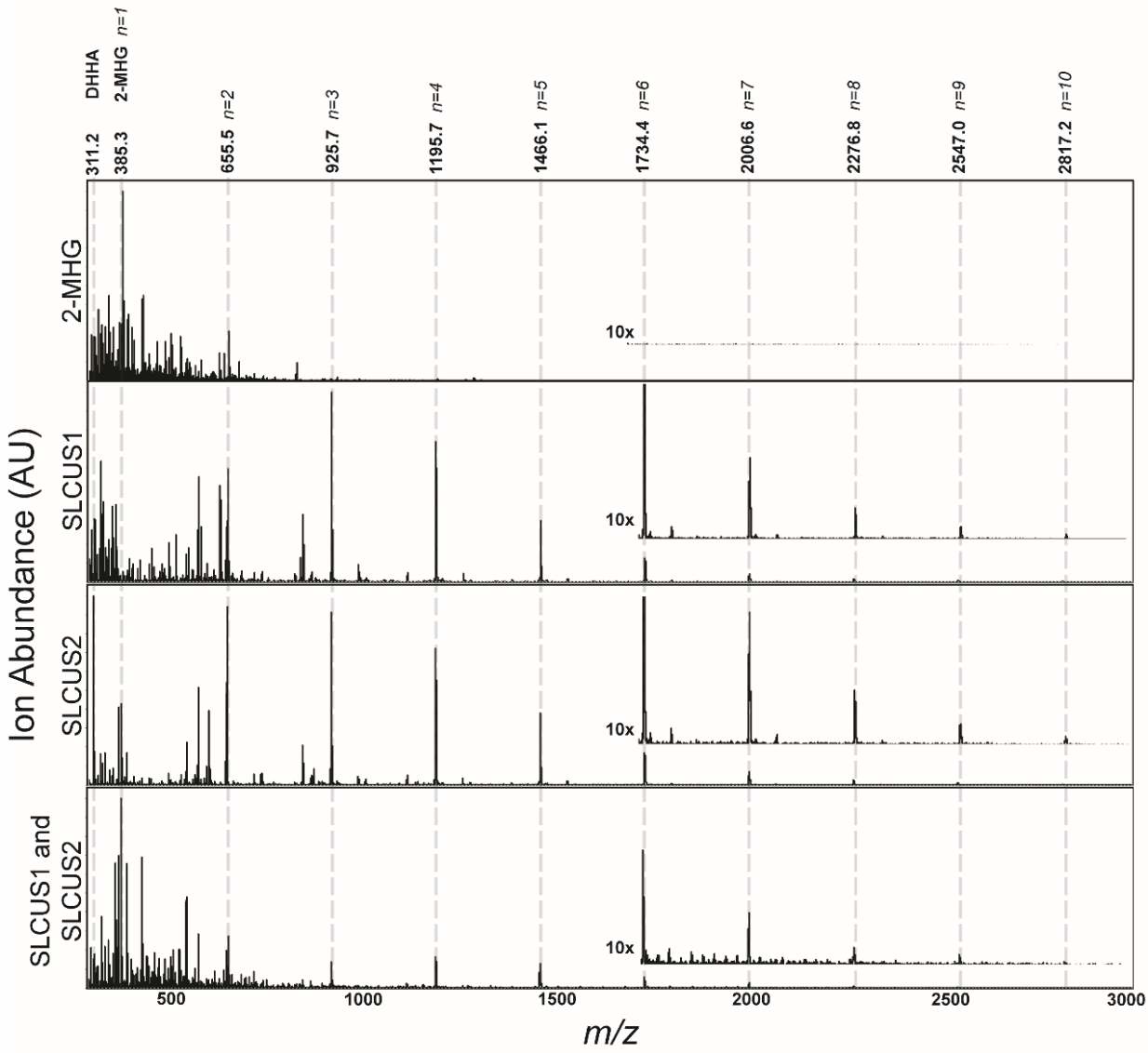

Figure 2.3. MALDI-TOF spectra of SLCUS1 and SLCUS2 products.

Predicted masses indicated above spectra are Na+ adducts of products. DHHA, is the hydrolysis product of 2-MHG. Insets are 10x magnifications of the spectra.

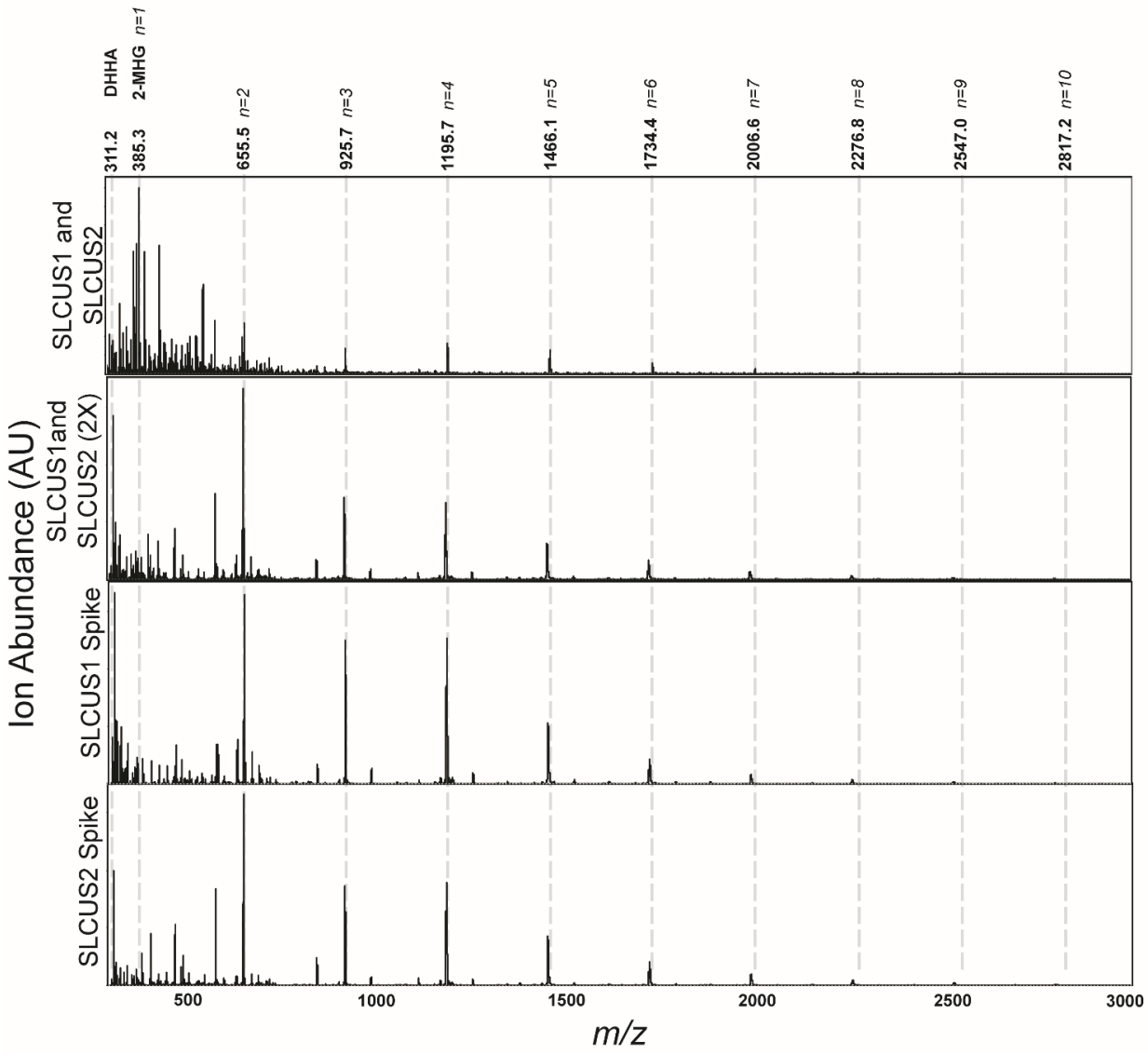

Figure 2.4. MALDI-TOF spectra of SLCUS1 and SLCUS2 products under various conditions.

Predicted masses indicated above spectra are Na+ adducts of products. DHHA, is the hydrolysis product of 2-MHG. Insets are 10x magnifications of the spectra. The first two spectra correspond to a co-incubation of SLCUS1 and SLCUS2 with 2-MHG, the first with 0.25 µg of each protein, the second with 0.5 µg of each protein. The second two are trials in which 0.25 µg of

SLCUS1 or SLCUS2 were incubated with 2-MHG for 12 hours before the addition of the second enzyme.

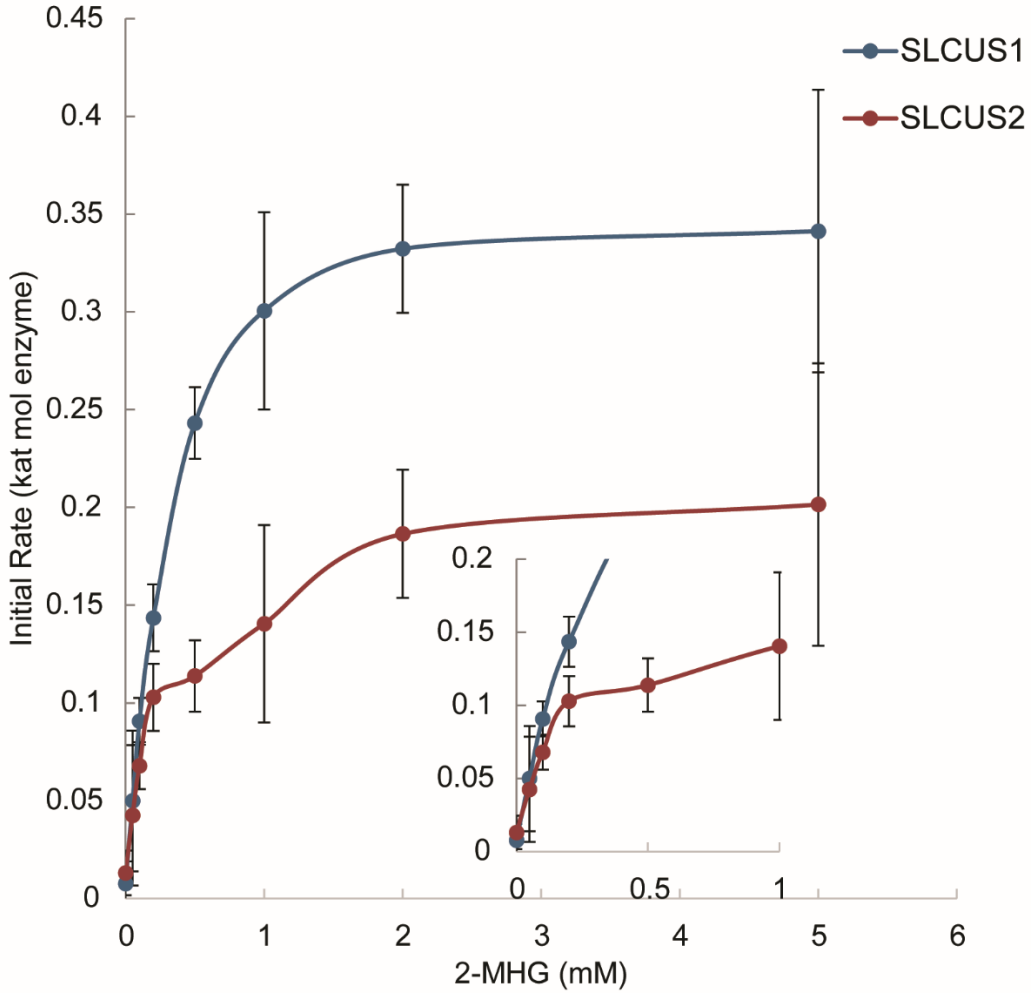

Figure 2.5. Kinetic characterization of SLCUS1 and SLCUS2. The effect of 2-MHG concentration on the initial reaction rate. Data were fitted to the Michaelis-Menten model as shown. Error bars represent the standard errors of three replicates.

	K_m (μM)	k_{cat} (s^{-1})	k_{cat}/K_m ($M^{-1}s^{-1}$)
SLCUS1	294 ± 24	0.375 ± 0.008	1275
SLCUS2	237 ± 62	0.198 ± 0.013	835
SLCUS1 (Yeats *et al*., 2014)	925 ± 98	0.314 ± 0.012	339

Table 2.1. Apparent Michaelis-Menten kinetics of SLCUS1 and SLCUS2.

Standard errors of kinetic parameters are given.

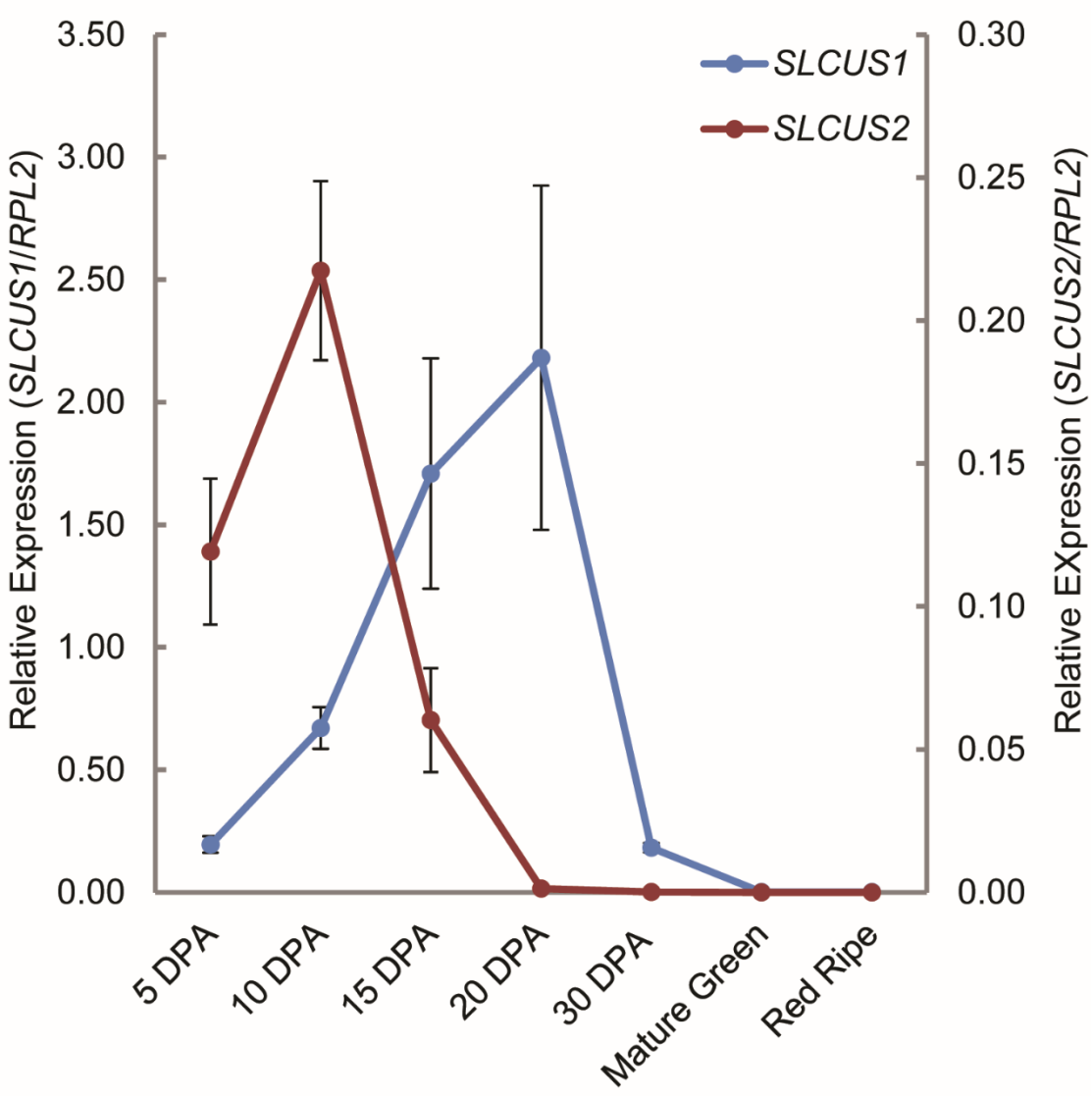

Figure 2.6. Expression of *SLCUS1* and *SLCUS2* in fruit. Expression of *SLCUS1* (left axis) and *SLCUS2* (right axis) relative to *RPL2* (Solyc10g006580). RNA was isolated from the total pericarp at the indicated stage. DPA = Days Post Anthesis. Error bars indicate the standard errors of three replicates.

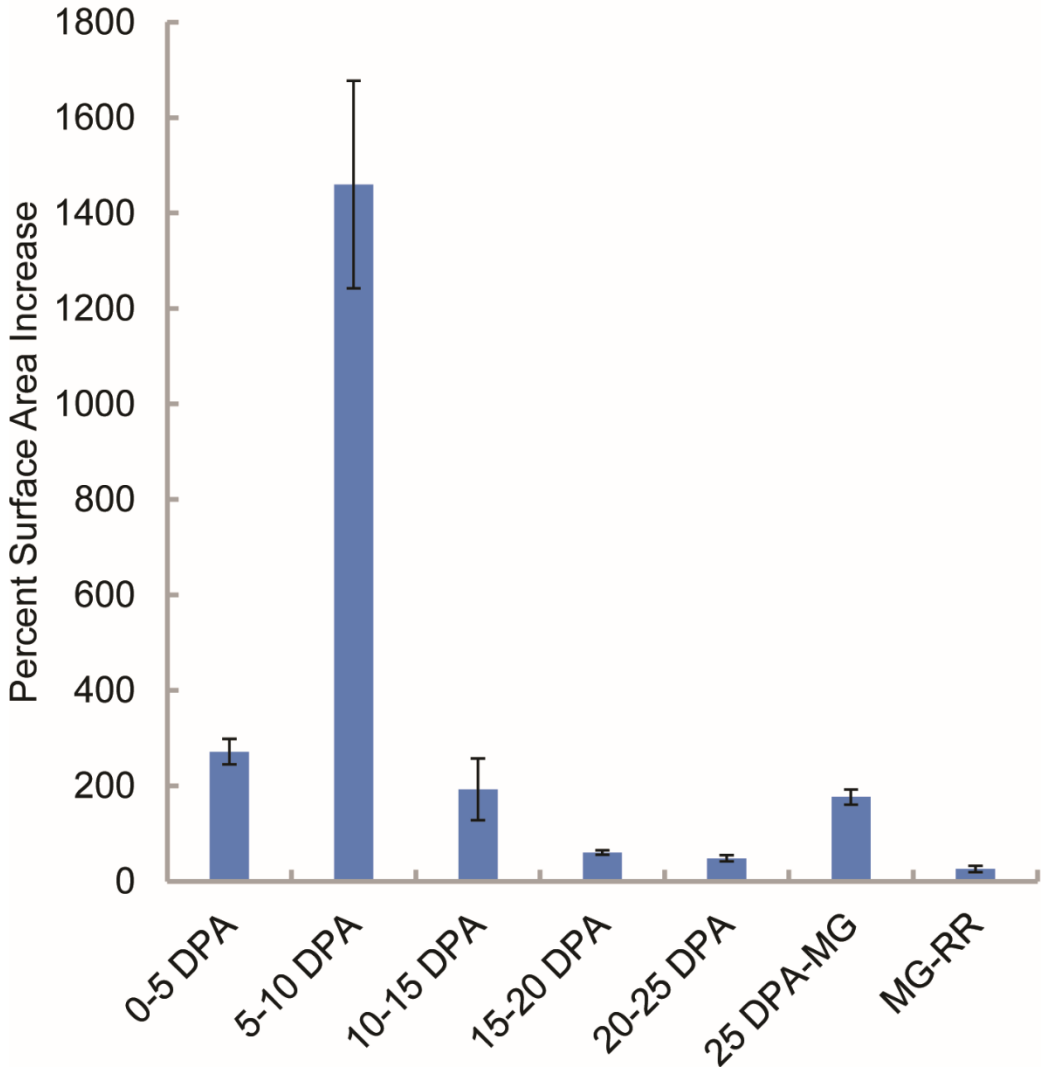

Figure 2.7. Increase in fruit surface area during development. Surface areas of 15 fruit were measured over the course of development. The percentage increase between developmental stages was calculated. DPA = days post anthesis, MG = Mature green, RR = Red Ripe. Error bars indicate the standard error of 15 replicates.

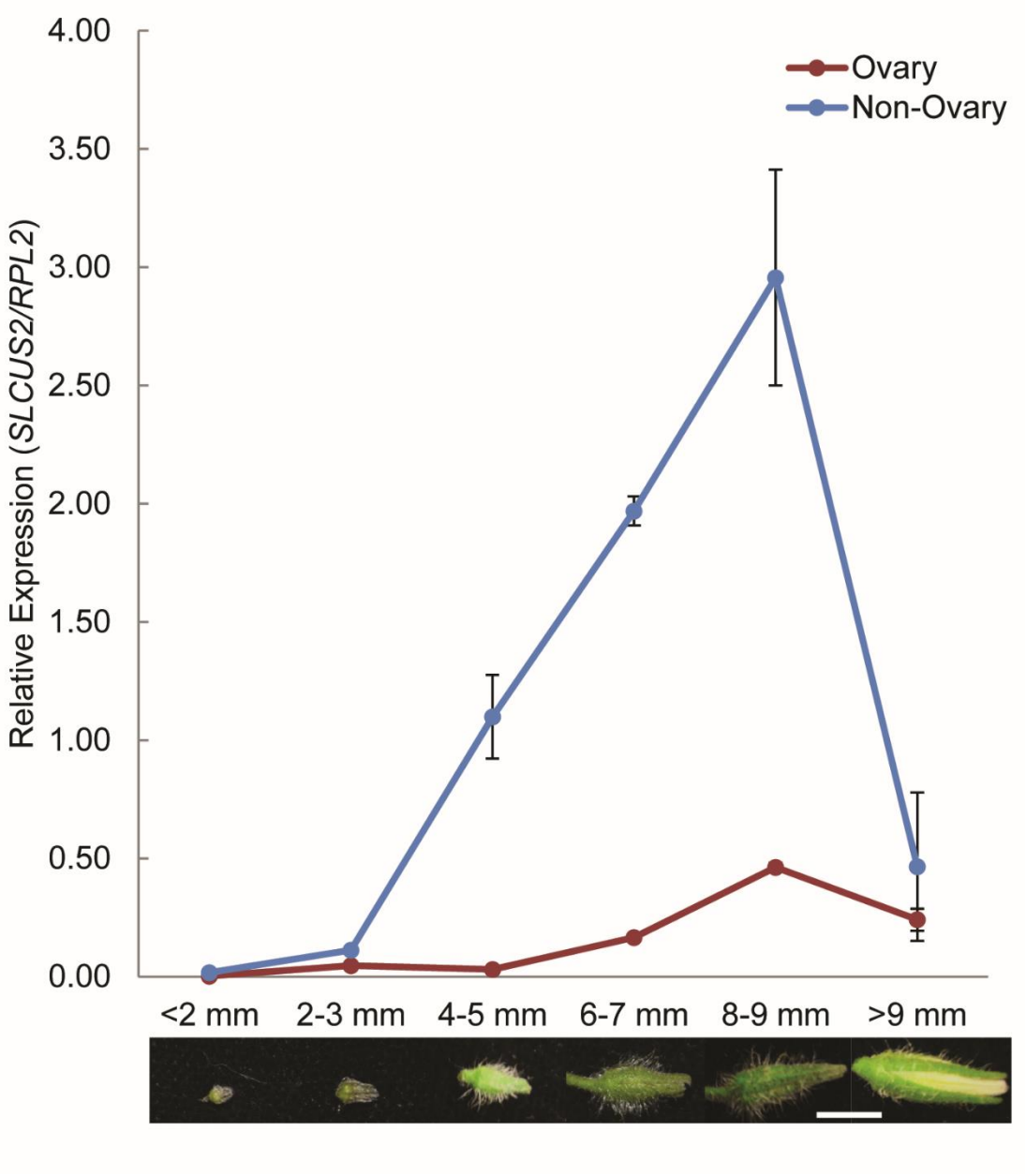

Figure 2.8. *SLCUS2* expression in dissected flowers during development. Expression was measured by qPCR after separating the ovaries from the remaining floral parts (sepals, anthers, and petals). Error bars indicate the standard errors of three replicates relative to *RPL2*. Scale bar is 5 mm.

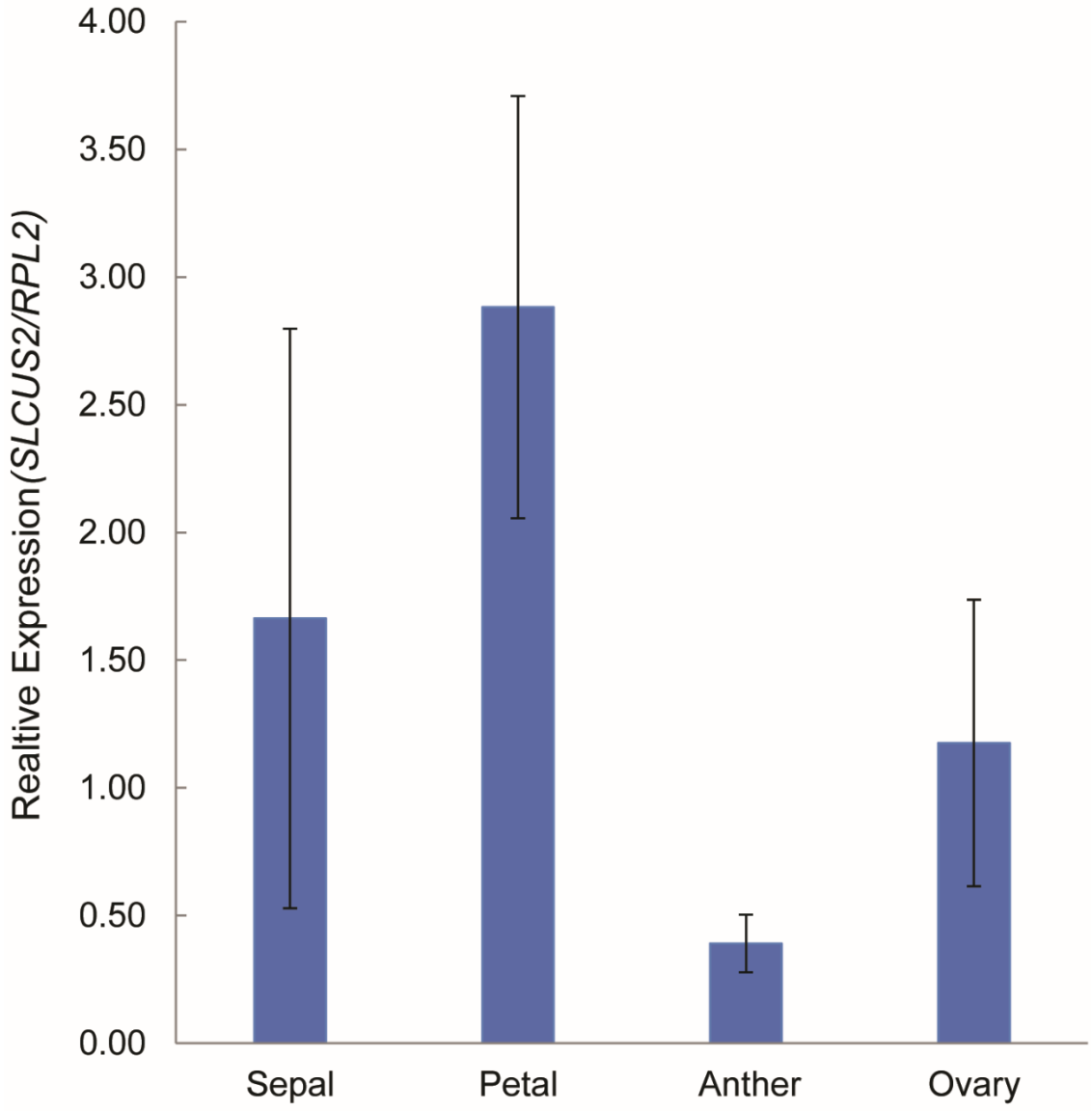

Figure 2.9. Expression of *SLCUS2* in floral organs. Expression of *SLCUS2* was evaluated in flowers at the 8-9 mm stage. Expression was compared relative to *RPL2*. Error bars indicate the standard error of three replicates. No statistical differences could be identified in the expression of *SLCUS2* between any organs using a t-test or a Tuckey's post-hoc test.

Figure 2.10. Mutation of CUS2 in *slcus2* Lines. Amino acid sequence alignment of wild type and *SLCUS2* CRISPR knock out (KO) lines. The CRISPR induced mutation results in a four base pair deletion resulting in a frameshift at residue 72 and a premature stop codon at residue 81.

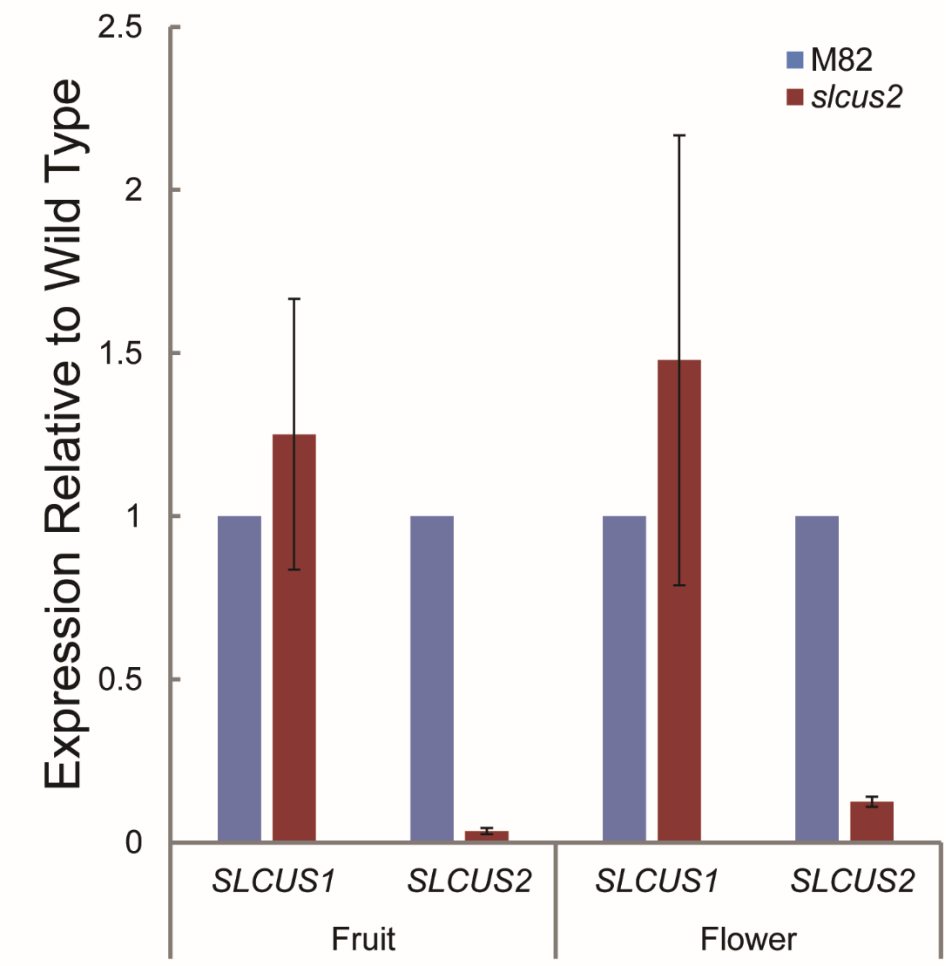

Figure 2.11. *SLCUS2* expression is decreased in *slcus2* lines. Expression of CUS1 and CUS2 relative to WT. For fruit analysis expression was determined at 10 days post anthesis (DPA). For flower expression RNA was isolated from 8-9 cm flowers. RPL2 was used as a reference gene. Error bars indicate the standard errors of three replicates.

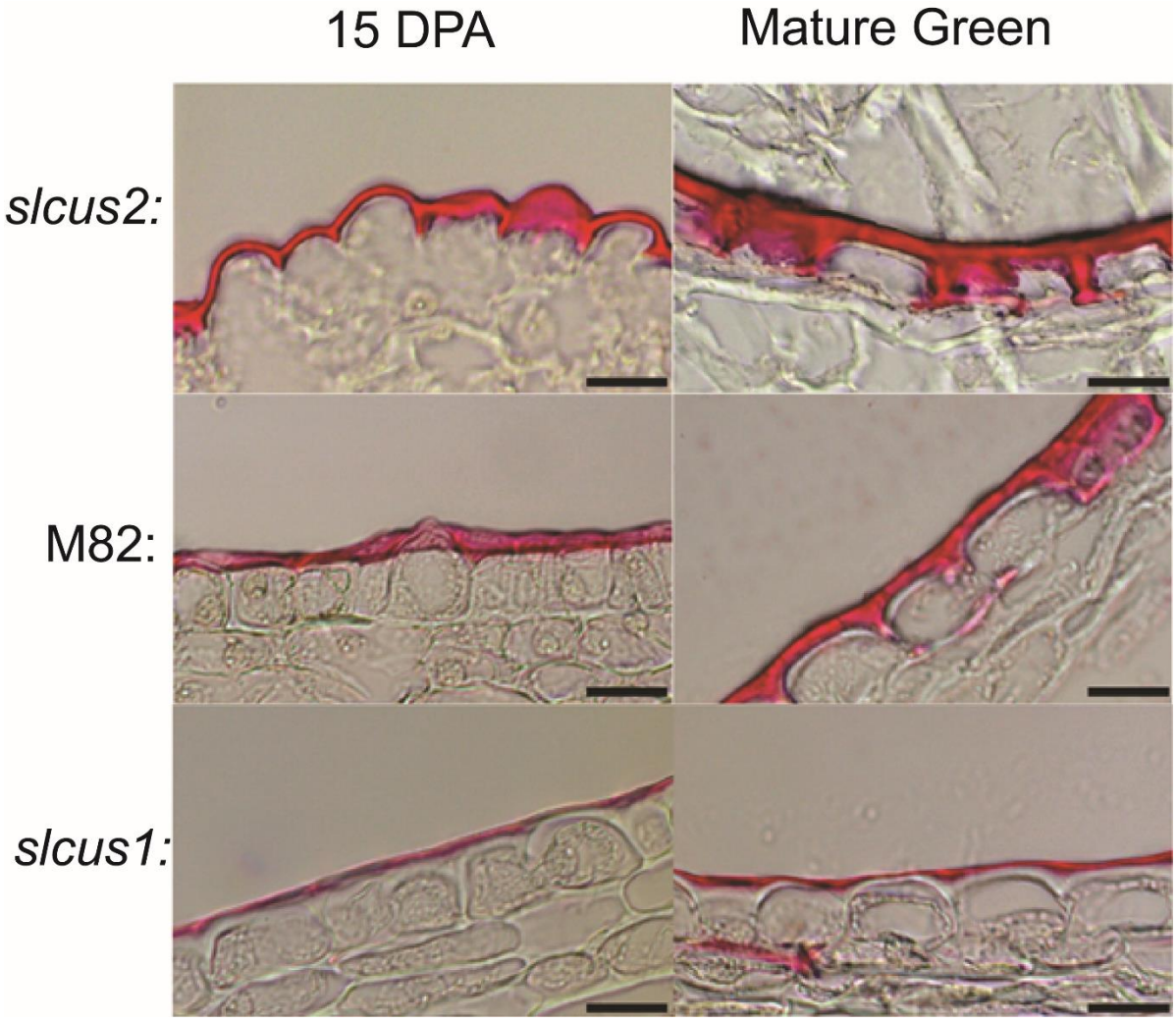

Figure 2.12. Lipid staining in M82, *slcus2*, and *slcus1* fruits. Oil Red O staining of the M82, *slcus2*, and slcus1 fruits during fruit development. Images on the left depict fruits pericarp sections stained at 15 days post anthesis (DPA). Images on the right depict sections stained at the mature green stage of development. Scales bars are 20 µm.

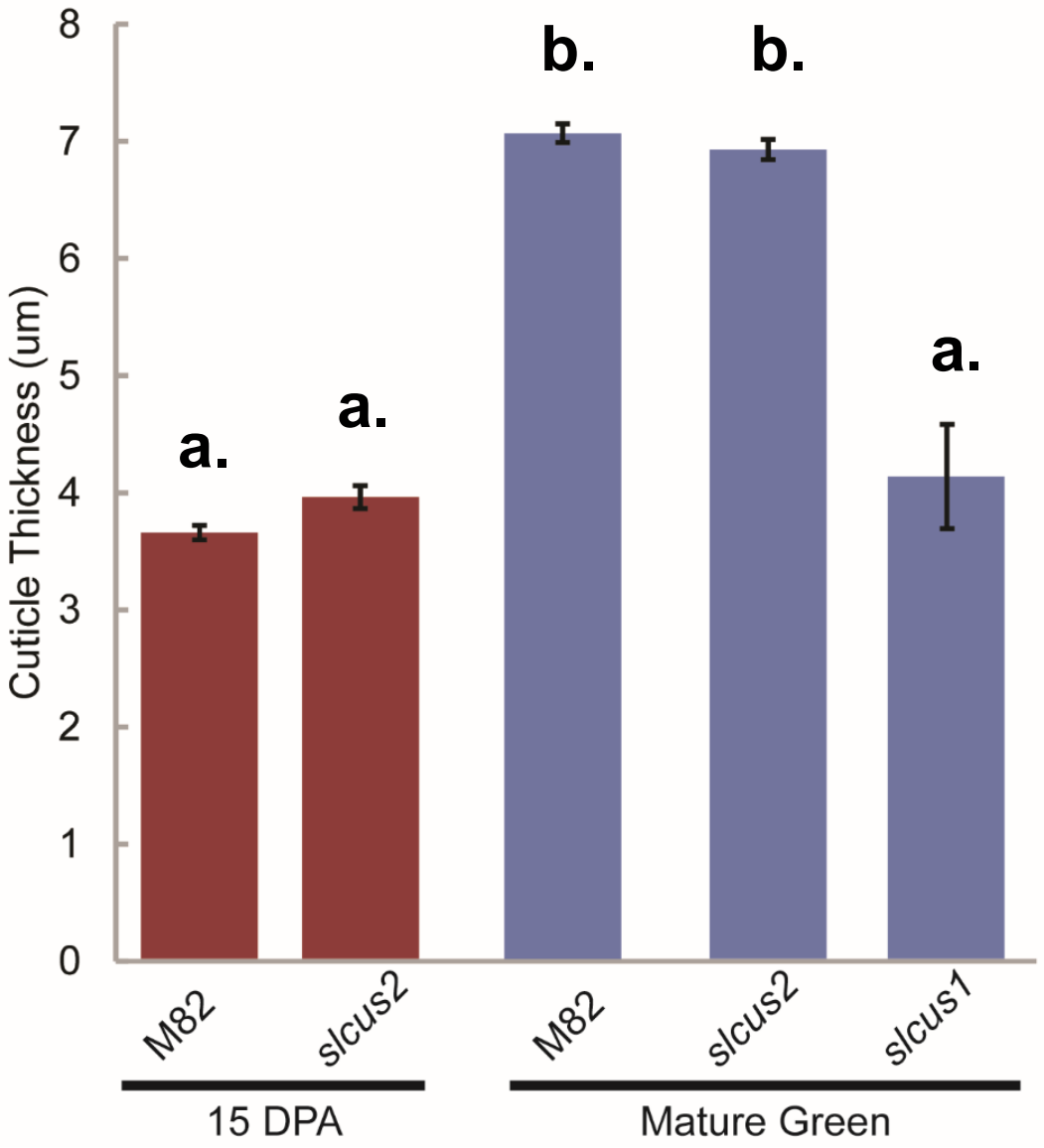

Figure 2.13. Cuticle thickness over fruit development. The thickness of the cuticle from the center of the epidermal cells was performed in ten different fruits at both 15 days post anthesis (M82 and *slcus2*) and mature green (M82, *slcus2*, and *slcus1*). Error bars indicate the standard error of 300 replicates, except for *slcus1*, which had 60 replicates. Letters indicate grouping based on statistically significant differences in cuticle thickness (Tukey's post-hoc test, $P<0.05$).

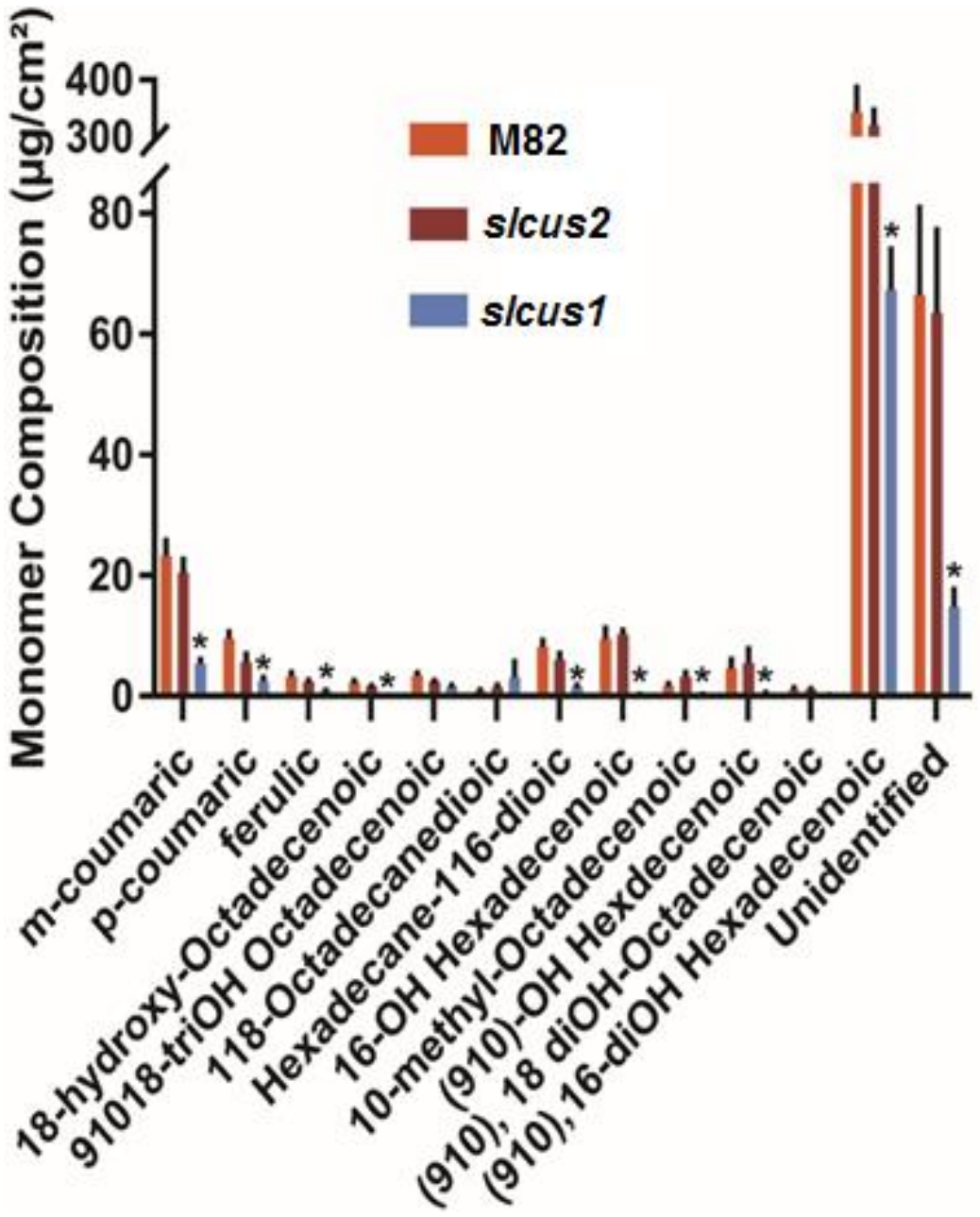

Figure 2.14. Chemical analysis of cutin monomer composition in M82, *slcus2*, and *slcus1*. GC-FID analysis of the monomer composition of mature

green fruits from M82, *slcus2*, and *slcus1* lines. Error bars indicate the standard error of ten replicates. Asterisks indicate statistically significant differences from M82 (t-test, $P<0.05$).

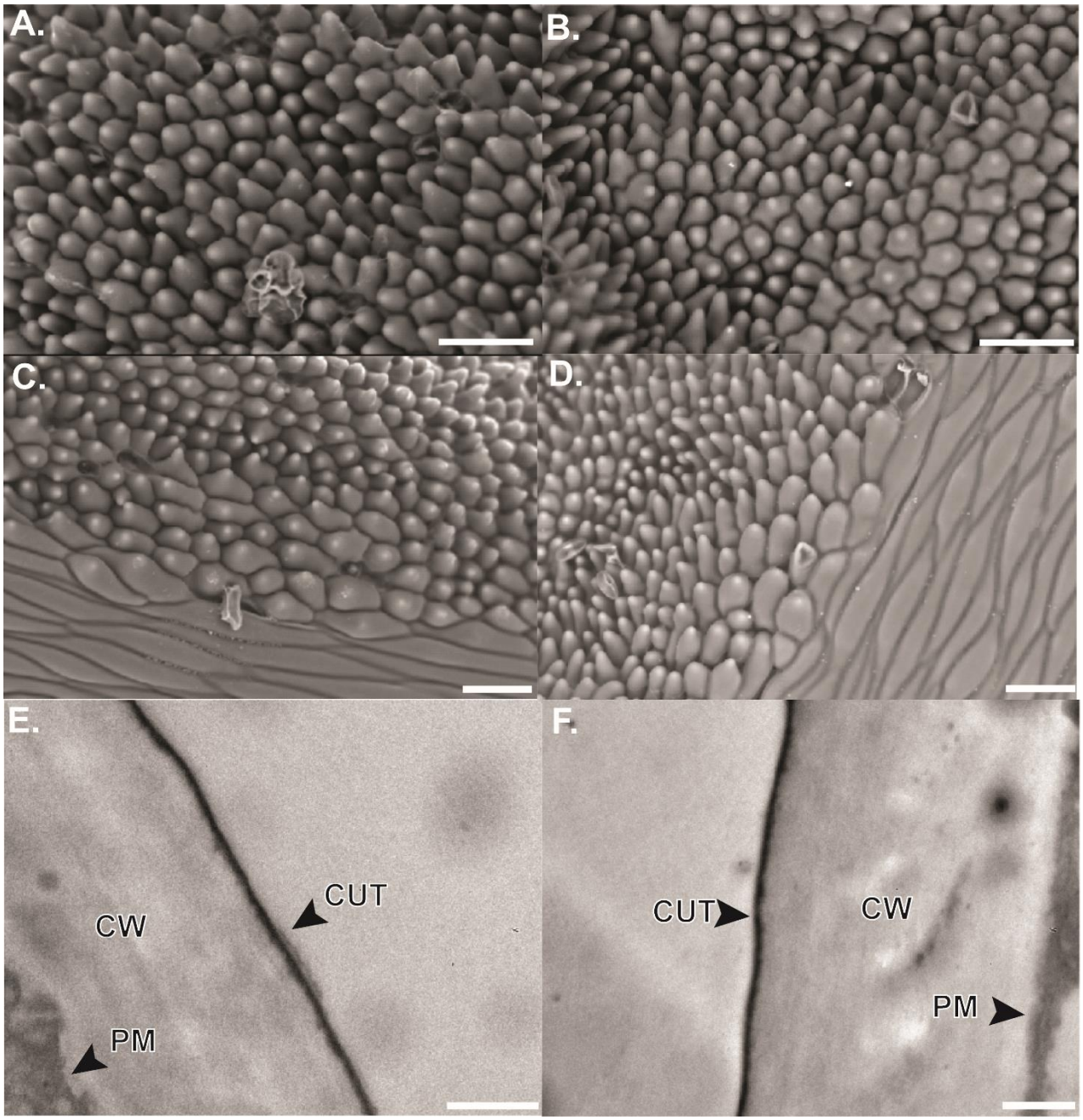

Figure 2.15. Electron microscopy of flower petals. Scanning electron microscopy of M82 (A and C) and *slcus2* (B and D) mature flower petals. Images C and D depict both flat and conical petal epidermis cells. Transmission electron microscope images of M82 (E) and *slcus2* (F) flower petals. Scale bars for A-D are 50 µm and scale bars for E-F are 500 nm.

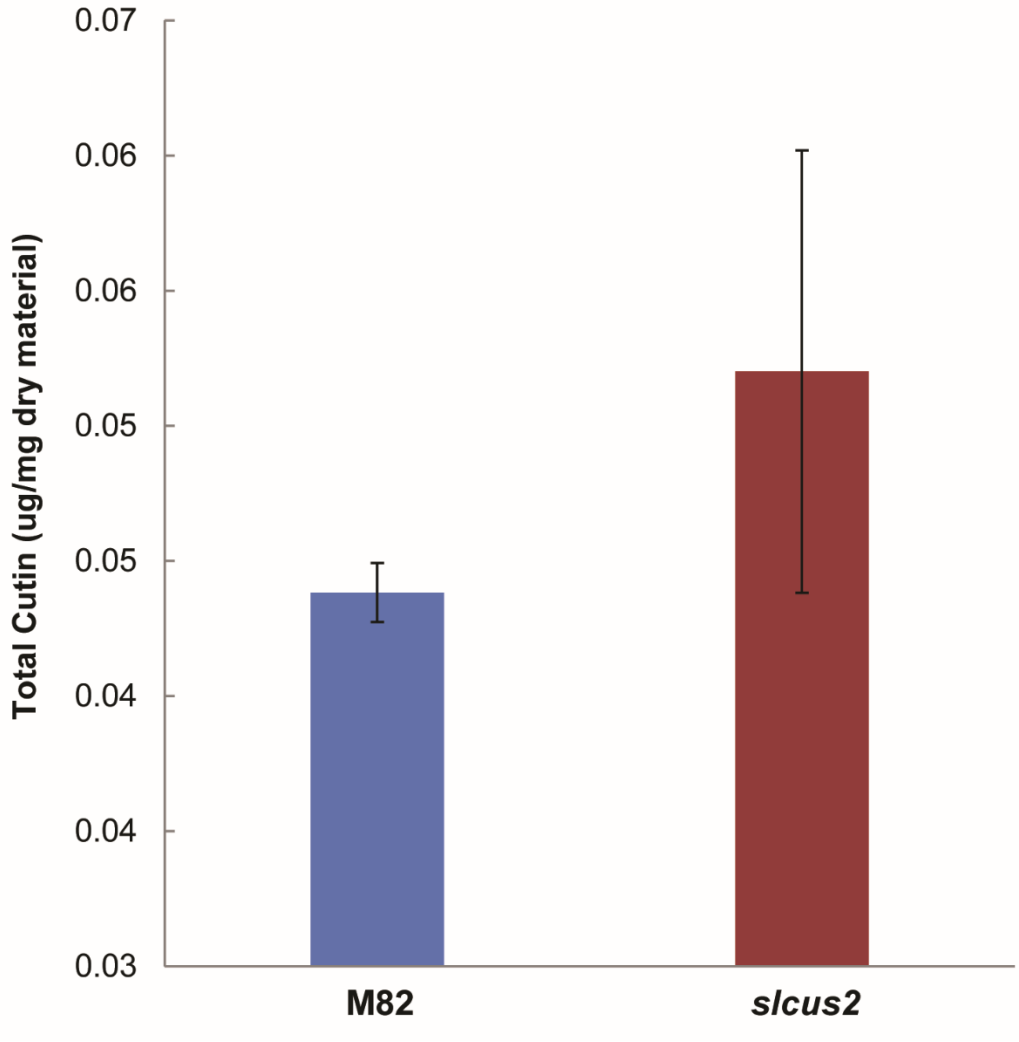

Figure 2.16. Chemical analysis of cutin from flower petals. GC-FID analysis of the total cutin (µg) per mg of petal material (mg). Error bars indicate the standard error of four replicates.

Materials and Methods

Expression from Tomato Expression and Generating Protein Models: Expression of the CUS genes were taken from the Tomato Expression Atlas (http://tea.sgn.cornell.edu) using the default settings focusing only on the pericarp tissues. Protein alignments were generated using Tree-based Consistency Objective Function for Alignment Evaluation (T-Coffee) (http://tcoffee.crg.cat/). Protein models were generated using Phyre2 (http://www.sbg.bio.ic.ac.uk/phyre2/html/page.cgi?id=index) using the default settings on the "normal" modelling mode after removing the predicated signal peptides. Models were colored using UCSF Chimera (https://www.cgl.ucsf.edu/chimera/).

Recombinant Expression/Purification, Kinetics, and MALDI: Recombinant SLCUS2 was expressed in *Nicotiana benthamiana* by amplifying the coding sequence of SLCUS2 using primers to remove the stop codon and incorporate *AgeI* and *SmaI* restriction sites. The resulting amplicon was inserted into the pEAQ-*HT* vector (Sainsbury *et al*. 2009). The pEAQ-*HT*::SLCUS2 was infiltrated into *N*. *benthamiana* with *Agrobacterium tumefaciens* strain GV3101. Plants were harvested 4 days after infiltration and leaves were flash frozen in liquid nitrogen and stored at -80 C.

For protein purification, 30 g of frozen leaves were homogenized using a mortar and pestle with 100 mL protein homogenization buffer (50 mM

Na_2HPO_4, 500 mM NaCl, 10mM sodium metabisulfite, pH 7.0). The homogenate was filtered through Miracloth (Millipore Sigma) and centrifuged at 10,000xg for 15 minutes at 4°C. The supernatant was decanted and the 1M sodium phosphate, pH 7.0 was added to a final concentration of 50 mM. 2M imidazole was added to a final concentration of 10mM. The centrifugation was repeated as before.

Following centrifugation, the supernatant was incubated with 200 µL of equilibrated HisPur Ni-NTA resin (Pierce) for 2 hours while rocking on ice. After 2 hours, the samples were spun at 700xg for 2 minutes at 4°C. The resin was transferred to a 5 mL column and washed with 5 mL of protein wash buffer (50 mM Na_2HPO_4, 500 mM NaCl, 50 mM imidazole, pH 7.0). Protein was eluted with 2 mL of protein elution buffer (50 mM Na_2HPO_4, 500 mM NaCl, 300 mM imidazole, pH 7.0).

Elute was applied to a size exclusion chromatography was performed using FPLC with a Superdex 75 HR 10/30 column (GE Healthcare Life Sciences) equilibrated with 100mM ammonium acetate (pH 7.0), 150mM NaCl at a flow rate of 0.5 ml/min. Fractions containing the recombinant protein were screened using a protein gel and collected and concentrated using a Vivaspin 6 column (10,000 MWCO, Sartorious Stedim Biotech, www.sartorius.com) that had been washed to remove glycerol from the filter.

Determination of kinetic parameters was determined in triplicate using 100 µL assays with the indicated 2-MHG concentrations, 150 mM NaCl, and 50 mM

sodium acetate (pH 5.0) at 37 °C. The reactions were initiated with either 80 ng of SLCUS1 or 160 ng of SLCUS2. Reactions were terminated by boiling for 10 minutes. 80 µL of each reaction was transferred to a microtiter plate and added to each sample was: 20 µL of 1 M sodium phosphate (pH 7.0) and 100 µL Free Glycerol Reagent. The samples were mixed and incubated at room temperature for 5 minutes. The absorbance at 560 mn was measured using a plate reader. For each reaction, a background was determined using boilied enzyme and subtracted before analysis. Fitting of the data to the Michaelis-Menten equation was performed using KaleidaGraph (Synergy Software).

For MALDI-TOF experiments, 5 mM 2-MHG was added to 50 mM ammonium acetate pH 4.5. To this, either 0.5 µg of CUS1, 0.5 µg CUS2, or 0.25 µg of both enzymes was added. In addition, controls in which the protein were boiled, or no 2-MHG was included for analysis. Reactions occurred at 37°C for 24 hours, after which the samples were diluted using three times the volume of methanol. 0.5 µl of the sample and 0.5 µl of matrix (10mg/ml DHB in 75% methanol/25 % H2O) were spotted onto a MALDI-TOF plate. The samples were dried at room temperature and the spectra was collected using a Waters MALDI Micro MX. Spectra was collected for each of the samples and the background (samples containing no 2-MHG) were subtracted using mMass3 software.

qPCR:

Total RNA was extracted from either the fruit pericarp or from floral tissue using the TRIzol® (Life Technology) method following the manufacturer's instructions. 1,500 ng of total RNA was digested using RQ1 DNase (Promega). cDNA was synthesized using a reverse transcription reaction (RNA to cDNA EcoDry Premix, Takara Bio). The quality of the cDNA was tested using primers for RPL2 (Solyc10g006580) using conventional PCR methods. Primers used for the qPCR were as followed: *RPL2*: forward: CAGCGGATGTCGTGCTATGAT, reverse: GGGATGCTCCACTGGATTCA; *SLCUS1*: forward: GTAGCATGTTGTGGACAAGGACCA, reverse: TTTGCCCTCTCAGATGGATGGAAC; *SLCUS2*: forward: CGAGCCTTCTTCGTGTTTG, reverse: ATGAGTAGGATAGTCAATGCC. qPCR was performed using Affymetrix HotStart-IT SYBR Green qPCR Master Mix and a Life Technology/ABI ViiA7 instrument using the standard run method in the ViiA 7 software. All reactions were performed using biological triplicates.

Surface Area Measurement:

For measuring the surface area, 15 fruits were taken at each stage indicated. The diameter of each fruit was measured at three places and the average was taken between the three measurements using digital calipers. The average of the three diameters was used to calculate the surface area, assuming the average diameter corresponds to a perfect sphere.

Generating CRISPR Lines (including screening):

CRISPR lines targeting *SLCUS2* were generated using two sgRNA target sites separated by 94 nucleotides, following a previously described protocol (Brooks *et al.*, 2014). Constructs: Level 1 (Addgene catalog number): pICH47732::NOSp::NPTII (51144), pICH47742::35s::Cas9 (49771), pICH47751::AtU6p::sgRNA1, pICH47761::AtU6p::sgRNA2, and pICH41780 (48019) as a linker. The level 1 vectors were assembled into the level 2 vector pAGM4723 (48015) using the Golden Gate cloning method (Weber *et al.*, 2011) The resulting vector was inserted through Agrobacterium tumefaciens-mediated transformation into calli generated from seeds from the M82 cultivar at the Boyce Thompson Institute, Ithaca NY. T0 lines were grown until seeds were collected. The T1 generation was screened for seedlings lacking the Cas9 insert followed by screening for homozygous deletions of *SLCUS2* using the following primers: Forward: TGCTTGCATTTTGTGATCTTCC, Reverse: ATTTTTATAGCCAAACGGATTCTC.

Electron Microscopy:

Scanning Electron Microscopy was performed using a JEOL 6480LV microscope using LV-cryo imaging. Live tissue was attached to a cryo-stage, flash frozen in liquid nitrogen, and imaged immediately. For transmission electron microscopy, petals were fixed with 1% gluteraldehye and 1% paraformaldehyde in 0.1 M Sorenson’s buffer pH 7.0 on ice for 60 minutes. Embedding and sectioning was performed as previously described

(Domozych, *et al.*, 2009). The sections were viewed with a Zeiss Libra 120 transmission electron microscope.

Light Microscopy:

Tissue fixation and embedding was performed as previously described (Buda *et al.*, 2009). A Microm HM550 cryostat (ThermoFisher Scientific) was create 8 micron sections of the pericarp. Sections were melted onto VistaVision Histobond (VWR) slides at room temperature. Oil Red O (Alfa Aesar) which had been supersaturated in isopropanol was filtered with a syringe filter with pore size 0.8/0.2 µm (Acrodisc® Syringe Filters, Pall Corporation) and diluted 3:2 with distilled water. The diluted solution rested for 30 minutes at room temperature and filtered again as above. Pericarp sections were incubated with diluted Oil Red O stain at 100% humidity for 30 min and rinsed with a gradient of 50%, 50%, 30%, 22%, 15%, and 8% isopropyl alcohol before being rinsed and mounted using distilled water. Sections were imaged using an AxioImager A1 microscope (Zeiss) using Zeiss EC-Plan NeoFluar 40x/0.75 dry and Zeiss ZEN 2012 blue edition software.

Cutin Chemical Analysis:

For analysis of the fruit cutin monomer composition, 10 biological replicates were analyzed. For each biological replicate, 0.3cm^3 discs were removed from fruits at the indicated developmental stage. The discs were treated with 2% (v/v) pectinase (EC 3.2.1.15; Sigma-Aldrich), 0.1% (v/v)

cellulose (EC 3.2.1.4; Sigma-Aldrich) in 50mM sodium citrate buffer (pH 4.0) containing 0.02% (w/v) sodium azide to prevent microbial growth. The discs were incubated at 40°C. The isolated cuticles were dewaxes by washing in chloroform, chloroform/methanol 1:1, and then methanol and dried under a gentle stream of nitrogen.

For the analysis of petal cutin monomers, the samples were delipidated as follows. Unless otherwise noted, all solutions contained 0.01% butylated hyoxytoluene and each extraction step took place while rocking at 250 rpm for at least an hour. 40 mL glass vials were filled with isoproponal and heated to 85°C. 100 mg of tomato flower petals from flowers between 8 and 9 mm long were immersed in the boiling isopropanol and shaken. The solvent was removed and the samples were extracted with fresh isopropanol. The solution was removed and replaced with chloroform/methanol (2:1, v/v) and shaken. The solution was removed and replaced with chloroform/methanol (1:2; v/v). The solution was removed and replaced with methanol and shaken. The methanol was removed and the samples were dried under a gentle stream of nitrogen gas at 40°C for 30 minutes. The samples were then dried using a Labconco Freezone 6 vacuum dessicator for 48 hours, until a constant weight was achieved.

The dewaxed samples were placed in a glass vial along with 50 µg of methyl heptadecanoate and ω-pentadecalactone to serve as internal standards. One mL of reaction mixture, containing 0.6 mL methanol, 0.15 methyl acetate, and 0.25 25% sodium methoxide, was added to the isolated

discs and the reaction vials were capped and heated to 60°C overnight. The following day, the samples were cooled to room temperature and 2 mL dichloromethane, 0.25 mL glacial acetic acid, and 500 µl 0.9% NaCl (w/v) Tris 100 mM pH 7.5. The samples were mixed and centrifuged for 2 minutes at 1500 xg. The upper phase was disposed of and the lower phase was washed with 1 mL 0.9% NaCl, mixed, and centrifuged. The upper phase was disposed of and water was removed from lower phase by the addition of anhydrous sodium sulfate and the solution was transferred to a clean reaction vial.

For derivatization, ~1/10 of each sample was transferred to a clean, conical reaction vial and evaporated to dryness under a gentle stream of nitrogen gas. 50 µL of BSTFA (Sigma-Aldrich) and 50 µL pyridine were added to the dried samples. The tubes were capped and incubated for 10 minutes at 90°C. Following incubation, the samples were dried under a gentle stream of nitrogen gas at 40°C. The samples were resuspended in 100 µL chloroform and transferred to an autosampler vial with glass insert (VWR). The samples were run on an Aligent 6850 gas chromatograph using a previously reported run protocol (Yeats *et al*., 2012).

REFERENCES

Akoh, C.C., Lee, G.C., Liaw, Y.C., Huang, T.H. and Shaw, J.F. (2004) GDSL Family of Serine Esterases/Lipases. *Prog. Lipid Res.* **43**, 534-552.

Baker, E.A., Bukovac, M. and Hunt, G.M. (1982) Composition of tomato fruit cuticle as related to fruit growth and development. In *The Plant Cuticle*, (Cutler D.F., Alvin K.L., Price C.E., eds) London: Academic Press, pp. 45-85.

Belhaj, K., Chaparro-Garcia, A., Kamoun, S. and Nekrasov, V. (2013) Plant genome editing made easy: targeted mutagenesis in model and crop plants using the CRISPR/Cas system. *Plant Methods* **9**, 39.

Brooks, C., Nekrasov, V., Lippman, Z.B. and Van Eck J. (2014) Efficient gene editing in tomato in the first generation using the CRIPSR/CAS9 system. *Plant Physiol.* **166**, 1292-1297.

Buda, G.J., Isaacson, T., Matas, A.J., Paolillo, D.J. and Rose, J.K.C. (2009) Three-dimensional imaging of the plant cuticle architecture using confocal scanning laser microscopy. *Plant J.* **60**, 378-385.

Chepyshko, H., Lai, C.P., Huang, L.M., Liu, J.H. and Shaw, J.F. (2012) Multifunctionality and discovery of GDSL esterase/lipase gene family in rice (*Oryza sativa* L. *japonica)* genome: new insights from bioinformatics analysis. *BMC Genomics* **13**, 309.

Deas, A.H.B. and Holloway, P.J. (1977) The intermolecular structure of some plant cutins. In *Lipids and Lipid Polymers in Higher Plants*, (Tevini M., Lichtenthaler H.K. eds.) Berlin: Springer, pp. 293–99.

Deshmukh, A.P., Simpson, A.J. and Hatcher, P.G. (2003) Evidence for crosslinking in tomato cutin using HRMAS NMR spectroscopy. *Phytochemistry* **64**, 1163–70.

Domínguez, E., Cuartero, J. and Heredia, A. (2011) An overview on plant cuticle biomechanics. *Plant Sci.* **181**, 77-84.

Domozych, D.S., Sorensen, I. and Willats, W.G. (2009) The distribution of cell wall polymers during antheridium development and spermatogenesis in the Charophycean green alga, Chara corallina. *Ann. Bot.* **104**, 1045-1056.

Edwards, D., Abbott, G.D. and Raven, J.A. (1996) Cuticles of early land plants: a paleoecophysiological evaluation. In *Plant Cuticles: An Integrated Functional Approach, (*Kersteinds G. ed.) Oxford, UK: BIOS, pp. 1-32.

Fich, E.A., Segerson, N.A. and Rose, J.K.C. (2016) The Plant Polyester Cutin: Biosynthesis, Structure, and Biological Roles. *Annu. Rev. Plant Biol.* **67**, 207-233.

Girard, A-L., Mounet, F., Lemaire-Chamley, M., Gaillard, C., Elmorjani, K., Vivancos, J., Runavot, J.L., Quemener, B., Petit, J., Germain, V., Rothan, C., Marion, D. and Bakan, B. (2012) Tomato GDSL1 is required for cutin deposition in the fruit cuticle. *Plant Cell* **24**, 3119-3134.

Holloway, P.J. (1982) Composition of tomato fruit cuticle as related to fruit growth and development. In *The Plant Cuticle*, (Cutler D.F., Alvin K.L., Price C.E., eds) London: Academic Press, pp. 45-85.

Hong, L., Brown, J., Segerson, N.A., Rose, J.K.C. and Roeder, A.H.K. (2017) CUTIN SYNTHASE 2 Maintains Progressively Developing Cuticular Ridges in *Arabidopsis* Sepals. *Mol. Plant.* **10**, 560-574.

Isaacson, T., Kosma, D.K., Matas, A.J., Buda, G.J., He, Y., Yu, B., Pravitasari, A., Batteas, J.D., Stark, R.E., Jenks, M.A. and Rose, J.K. (2009) Cutin deficiency in the tomato fruit cuticle consistently affects resistance to microbial infection and biomechanical properties, but not transpirational water loss. *Plant J.* **60**, 363-377.

Kelley, L.A., Mezulis, S. and Yates, C.M. (2015) The Phyre2 Web Portal for Protein Modeling, Prediction and Analysis. *Nat. Protoc.* **10**, 845-858.

Kolattukudy, P.E. (1977) Lipid polymers and associated phenols, their chemistry, biosynthesis, and role in pathogenesis. *Recent Adv. Phytochem.* **77**, 185–246.

Krolikowski, K.A., Victor, J.L., Wagler, T.N., Lolle, S.J. and Pruitt, R.E. (2003) Isolation and characterization of the Arabidopsis organ fusion gene HOTHEAD. *Plant J.* **35**, 501–511.

Kutschera, U. and Niklas, K.J. (2007). The epidermal-growth-control theory of stem elongation: an old and new perspective. *Planta* **170**, 168-80.

Li-Beisson, Y., Shorrosh, B., Beisson, F., Andersson, M.X., Arondel, V., Bates, P.D., Baud, S., Bird, D., DeBono, A., Durrett, T.P., Franke,

R.B., Graham, I.A., Katayama, K., Kelly, A.A., Larson, T., Markham, J.E., Miquel, M., Molina, I., Nishida, I., Rowland, O., Samuels, L., Schmid, K.M., Wada, H., Welti, R., Xu, C., Zallot, R. and Ohlrogge, J. (2013) Acyl-lipid metabolism. In The *American Society of Plant Biologists*, eds, The Arabidopsis Book 11:e0161.

López-Casado, G., Matas, A.J., Domínguez, E., Cuartero, J. and Heredia, A. (2007) Biomechanics of isolated tomato (*Solanum lycopersicum* L.) fruit cuticles: the role of the cutin matrix and polysaccharides. *J. Exp. Bot.* **58**, 3875-3883.

Matas, A.J., Yeats, T.H., Buda, G.J., Zheng, Z., Chatterjee, S., Tohge, T., Ponnala, L., Adato, A., Aharoni, A., Stark, R., Fernie, A.R., Fei, Z., Giovannoni, J.J. and Rose, J.K.C. (2011) Tissue- and Cell- Type Specific Transcriptome Profiling of Expanding Tomato Fruit Provides Insights into Metabolic and Regulatory Specialization and Cuticle Formation. *Plant Cell* **23**, 3893-3910.

Martin, L.B.B., Romero, F., Fich, E.A., Domozych, D.S. and Rose J.K.C. (2017) Cuticle biosynthesis is developmentally regulated by abscisic acid. *Plant Physiol.* **DOI:** 10.1104/pp.17.00387.

Sainsbury, F., Thuenemann, E.C. and Lomonossoff, G.P. (2009) pEAQ: versatile expression vectors for easy and quick transient expression of heterologous proteins in plants. *Plant Biotechnol. J.* **7**, 682-693.

Samuels, l., Kunst, L. and Jetter, R. (2008) Sealing plant surfaces: cuticular wax formation by epidermal cell. *Annu. Rev. Plant Biol.* **59**, 683-707.

Schreiber, L. (2010) Transport barriers made of cutin, suberin and associated waxes. *Trends Plant Sci.* **15**, 546–553.

Segado, P., Domínguez, E. and Heredia, A. (2016) Ultrastructure of the epidermal cell wall and cuticle of tomato fruit (*Solanum lycopersicum* L.) during development. *Plant Physiol.* **170**, 935-946.

Shi, J.X., Malitsky, S., De Oliveira, S., Branigan, C., Franke, R.B., Schreiber, L. and Aharoni, A. (2011) SHINE transcription factors act redundantly to pattern the archetypal surface of Arabidopsis flower organs. *PLoS Genet.* **7**, e1001388.

Shinozaki, Y., Nicholas, P., Fernandez-Pozo, N., Ma, Q., Evanich, D.J., Shi, Y., Xu, Y., Zheng, Y., Snyder, S.I., Martin, L.B.B., Ruiz-May, E., Thannhauser, T.W., Chen, K., Domozych, D.S., Catala, C., Fei, Z., Mueller, L.A., Giovannoni, J.J. and Rose, J.K.C. (2018) High-resolution spatiotemporal transcriptome mapping of tomato fruit development and ripening. *Nat. Commun.* **9**, 364.

Tsubaki, S., Ozaki, Y., Yonemori, K. and Azuma, J. (2012) Mechanical properties of fruit-cuticular membranes isolated from 27 cultivars of Diospyros kaki Thunb. *Food Chem.* **132**, 2135–2139.

Upton, C. and Buckley, J.T. (1995) A new family of lipolytic enzymes? *Trends Biochem. Sci.* **20**, 178-179.

Weber, E., Gruetzner, R., Werner, S., Engler, C. and Marillonnet, S. (2011) Assembly of designer TAL Effectors by Golden Gate Cloning. *PLoS One* **6**.

Yang, W., Simpson, J.P., Li-Beisson, Y., Beisson, F., Pollard, M. and Ohlrogge, J.B. (2012) A land-plant-specific glycerol-3-phosphate acyltransferase family in Arabidopsis: Substrate specificity, sn-2 preference, and evolution. *Plant Physiol.* **160**, 638–652.

Yeats, T.H., Huang, W., Chatterjee, S., Viart, H.M.F., Clausen, M.H., Stark, R. E., Rose, J.K.C. (2014) Tomato Cutin Deficient 1 (CD1) and putative orthologs comprise an ancient family of cutin synthase-like (CUS) proteins that are conserved among land plants. *Plant J.* **77**, 667–675.

Yeats, T.H., Martin, L.B.B., Viart, H.M.F., Isaacson, T., He, Y., Zhao, L., Matas, A.J., Buda, G.J., Domozych, D.S., Clusen, M.H. and Rose, J.K.C. (2012) The identification of cutin synthase: formation of the plant polyester cutin. *Nat. Chem. Biol.* **8**, 609-611.

Yeats, T.H. and Rose, J.K.C. (2013) The formation and function of plant cuticles. *Plant Physiol.* **163**, 5–20.